# Development of Dynamical and Mathematical Models
# of Exhausted Plasma Plumes and Plasmoids in Space


FINAL REPORT


Codes and Calculations


EOARD Contract SPC-94-4081


Principal Investigator

V. I Garkusha


Kaliningrad, Moscow region


1995

# REPORT DOCUMENTATION PAGE

Form Approved OMB No. 0704-0188

Public reporting burden for this collection of information is estimated to average 1 hour per response, including the time for reviewing instructions, searching existing data sources, gathering and maintaining the data needed, and completing and reviewing the collection of information. Send comments regarding this burden estimate or any other aspect of this collection of information, including suggestions for reducing this burden to Washington Headquarters Services, Directorate for Information Operations and Reports, 1215 Jefferson Davis Highway, Suite 1204, Arlington, VA 22202-4302, and to the Office of Management and Budget, Paperwork Reduction Project (0704-0188), Washington, DC 20503.

| 1. AGENCY USE ONLY (Leave blank) | 2. REPORT DATE 1995 | 3. REPORT TYPE AND DATES COVERED Final Report |
|---|---|---|

**4. TITLE AND SUBTITLE**

Development of Dynamical and Mathematical Models of Exhausted Plasma Plumes and Plasmoids in Space

**5. FUNDING NUMBERS**

F6170894W0795

**6. AUTHOR(S)**

Dr. Valery Garkusha

**7. PERFORMING ORGANIZATION NAME(S) AND ADDRESS(ES)**

Research Institute of Machine Building
4 Pioneerskaja St
Kalingrad, Moscow Region 141070
Russia

**8. PERFORMING ORGANIZATION REPORT NUMBER**

N/A

**9. SPONSORING/MONITORING AGENCY NAME(S) AND ADDRESS(ES)**

EOARD
PSC 802 BOX 14
FPO 09499-0200

**10. SPONSORING/MONITORING AGENCY REPORT NUMBER**

SPC 94-4081

**11. SUPPLEMENTARY NOTES**

**12a. DISTRIBUTION/AVAILABILITY STATEMENT**

Approved for public release; distribution is unlimited.

**12b. DISTRIBUTION CODE**

A

**13. ABSTRACT (Maximum 200 words)**

This report results from a contract tasking Research Institute of Machine Building as follows: Develop dynamic and mathematical models of explasma plumes and plasmoids in the space environment.

**14. SUBJECT TERMS**

EOARD

**15. NUMBER OF PAGES**

**16. PRICE CODE**

N/A

| 17. SECURITY CLASSIFICATION OF REPORT | 18. SECURITY CLASSIFICATION OF THIS PAGE | 19. SECURITY CLASSIFICATION OF ABSTRACT | 20. LIMITATION OF ABSTRACT |
|---|---|---|---|
| UNCLASSIFIED | UNCLASSIFIED | UNCLASSIFIED | UL |

NSN 7540-01-280-5500

Standard Form 298 (Rev. 2-89)
Prescribed by ANSI Std. 239-18
298-102

Valery I. Garkusha
Research Institute of Machine Building,
Pionerskaja  st., 4,
Kaliningrad, 141070, Moscow region,


December_____, 1995


Victoria H. COX,
EUROPEAN OFFICE
OF AEROSPACE RESEARCH AND DEVELOPMENT,
223/231 Old Marylebone Road,
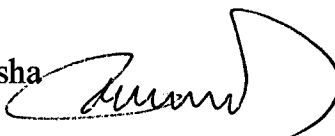London NW1 5TH

**Dear Ms. Cox,**

Thank You very much for Your last Fax dated 24 Nov 95.

I apologize for the long delay with submittance of our final deliverables according to EOARD Contracts SPC-94-4080 and SPC-94-4081. Being recently reorganized the ordinary routine to get all necessary permissions for the Institutes' issues took unexpectedly much time. We were wrong in evaluation of resulting time delay and understand our fault.

The Reports presented are added with diskette containing PC program products developed with .EXE files to make the Programs run as it was specified when You visited TsNIIMASH.

Best wishes with hope that this message is not our final contact,


Valery  Garkusha

## Abstract

The present report is the third and final deliverable according to EOARD Contract SPC-94-4081, item 0003.

The paper contains the dynamical problem solutions for certain thermal modes of artificial plasma expansion in space, codes to calculate the parameters of freely expanding plasma jet and plasmoid, representative samples of calculations, comparison of theoretical results obtained with data of measurements in plumes of electric and conventional gas thrusters, comparison of self-similar solutions obtained with published data of analytical and numerical calculation of parameters for plasma and gas jets.

## Nomenclature

| | | |
|---|---|---|
| a, l | = | transverse and longitudinal spatial scales of plasma jet |
| e | = | ion charge |
| $k=(a'_0)^{-2}$ | = | factor of flow divergency |
| M | = | Mach number |
| $\Pi$ | = | dimensionless criterion |
| m | = | ion mass |
| $\dot{N}$ | = | particles flow rate |
| n | = | particles concentration |
| T | = | temperature |
| x, r, $\varphi$ | = | cylindrical coordinates |
| u, $\nu$ | = | x- and r- components of flow velocity |
| V | = | flow velocity |
| $\gamma$ | = | specific heat ratio |
| $\lambda$ | = | mean free path |
| $6$ | = | plasma electric conductivity |
| $\eta = r/a$ | = | self-similar variable |
| $\nu$ | = | numerical multiplier |
| C | = | separation constant |

Subscripts:

| | | |
|---|---|---|
| "$_c$" | = | quantity at flow axis |
| "$_m$" | = | maximal quantity |
| "$_0$" | = | initial quantity |

*Prime* "'" denotes spatial along axis x derivatives.

Content:


## Introduction


## 1. Representative thermal modes of plasma Free Expansion

## 2. Program and Calculation of Plasma free Expansion

## 3. Comparison of results obtained with available data on Plasma and Gas free Expansion

## Discussion


## Conclusion


## References

# Introduction

The objectives of the work is development of dynamical and mathematical models of exhausted plasma plumes and plasmoids in space with due regard for actions of inner electric fields and thermal conductivity in plasma.

These models are intended to predict the behavior of artificial plasma formations (APF) arising in space particularly in vicinity of a spacecraft as the typical result of normal operation of certain onboard systems including electric thrusters both steady state and pulse operation , plasma contactors for tether systems and for spacecraft charging control as well as during active experiments. Knowledge of the APF characteristics is important for determination of communication, navigation and ranging conditions , for evaluation of APF influence on spacecraft environment and consequently on sensitive onboard equipment operation as well as for active experiments planning and data processing.

The previous intermediate report submitted as the second deliverable according to EOARD Contract SPC-94-4081, item 0002, contains dynamical problem formulation, general and particular solutions describing evolution of artificial plasma formations injected from a spacecraft and a brief description of algorithms and code under development for calculation of spatial and temporal plasma properties distributions in the frame of Development of Dynamical and Mathematical Models of Exhausted Plasma Plumes and Plasmoids in Space.

The dynamical problem describing evolution of both fully ionized stationary supersonic plasma jet and plasmoid is formulated and solved in a self-similar form. The basic idea of this approach is that a non-uniform plasma or gas flow tends "to forget its history", i.e. initial conditions, so that the latter becomes actually insufficient for flow expansion far from the source. Because of subsequent reasonable simplification the input combined partial differential equations of two components plasma dynamics were rearranged in a set of separable equations so that the problem was reduced to quadratures and to solution of ordinary nonlinear differential equations.

For practically interesting cases of plasma jet with uniform temperature or enthalpy in the flow cross sectional plane the solution was obtained in a simple analytic form.

The most noticeable feature of three dimensional plasmoid expansion is the inversion of its shape.

# 1. Representative thermal modes of plasma Free Expansion

## 1.1 Adiabatic plasma or gas jet expansion

In the previous intermediate report [1] the dynamical problem describing expansion of fully ionized stationary plasma jet is formulated and solved in a self-similar form. For two-dimensional supersonic plasma jet of low divergency, the variables x and r in the final set of dynamical equations separates.

The self-similar form of solution for this problem is written as:

$u = u_c(x) \cdot y(\eta)$; $v = u \cdot da/dx \cdot \eta$; $T = T_c(x) \cdot \tau(\eta)$; $nu = f(\eta) \cdot \dot{N}v /\pi a^2$.

where r = a(x) is a certain flow current line.

It was found that all dissipative effects mentioned above may be evaluated using the only dimensionless criterion

$$\Pi = \frac{6 T_e \pi a a'}{e^2 \dot{N}}$$

Here "a" is a spatial scale of plasma jet transverse size.
For the condition of

$$\Pi \ll 1$$

the combined equations (6) of report [1] may be rearranged to:

$$\frac{u^2}{u_0{}^2} = 1 + \frac{2}{(\gamma-1)M_0{}^2} \left( 1 - \frac{T}{T_0} \right); \tag{1.1}$$

$$u a' (u a')' = C \cdot T/m \cdot a'/a \tag{1.2}$$

$$\left( \frac{T_c}{T_0} \right)^{1/(\gamma-1)} \frac{u_c a^2}{u_0 a_0{}^2} = 1 \tag{1.3}$$

$$\frac{T_c u_0 a_0{}^{2-C}}{T_0 u_c a^{2-C}} = 1 \tag{1.4}$$

$$\frac{\tau}{y^2} = 1 + \eta^2 \tag{1.5}$$

$$f y = \frac{1}{(1 + \eta^2)^{1+C/2}} \tag{1.6}$$

Here C is free separation constant for variables x and $\eta = r/a$.

The equations 1.1, 1.2, 1.5 and 1.6 result from equations of motion for coordinates x and r, expression 1.3 represents equation of energy and expression 1.4 is the separation condition for variables x and $\eta$. The equations 1.1, 1.3 and 1.4 yield relationships:

$$T/T_0 = 1 - (u^2/u_0^2 - 1) \cdot M^2 \cdot (\gamma-1)/2$$

$$T/T_0 = (u^2/u_0^2)^{C(\gamma-1)/2(2\gamma-C)}$$

for $u^2/u_0^2 \ll 1$ $\qquad$ $T/T_0 \approx 1 + (u^2/u_0^2 - 1) \cdot \dfrac{C(\gamma-1)}{2(2\gamma-C)}$

Therefore the separation condition 1.4 is consistent with equations 1.1 and 1.3 if

$$C = \frac{2\gamma M_0^2}{M_0^2 - 1} \quad \text{and} \quad \frac{u^2}{u_0^2} - 1 = \frac{2}{(\gamma-1)M_0^2}\left(1 - \frac{T}{T_0}\right) \ll 1$$

The solution obtained is valid for conditions $u \neq$ const with $M_0^2 \gg 1$, i.e. for more wide range of jet parameters than that presented in report [1].

Finally the following jet parameters distributions for $M_0^2 \gg 1$ are obtained:

$$nu^2 = \frac{N \cdot \nu \cdot u_c}{\pi a^2} \frac{1}{(1+r^2/a^2)^{\,p+1}} ;$$

$$\frac{u_c^2}{u_0^2} = 1 + \frac{2}{M_0^2(\gamma-1)}\left[1 - \left(\frac{a_0^2}{a^2}\right)^q\right] \approx \left(\frac{a^2}{a_0^2}\right)^{2/(M^2-1)} ;$$

$$nT = \frac{N \cdot \nu \cdot T_c}{\pi a^2 u_c} \frac{1}{(1+r^2/a^2)^{\,p}} ;$$

$$\nu = u\,(1 + a'^2 \cdot r^2/a^2) ;$$

$$a'^2 = \frac{a_0'^2 + 2/((\gamma-1)\cdot M_0^2)\cdot[1-(a_0^2/a^2)^q]}{1 + 2/((\gamma-1)\cdot M_0^2)\cdot[1-(a_0^2/a^2)^q]} = 1-(1-a_0'^2)\frac{u_0^2}{u^2}$$

$$p = \gamma M_0^2/(M_0^2-1); \quad \nu=p-1/2 ; \quad q = \frac{(\gamma-1)M_0^2}{M_0^2 - 1}$$

As $a/a_0 \gg 1$ or for $M_0^2 \to \infty$ this solution is identical to that presented in report [1] for conically expanding jet.

## 1.2 Isothermal expansion of ion beam

Operation of onboard Stationary plasma (SPT) or Anode layer (TAL) electric thrusters results in arising in space of expanding ion beam with the following representative initial parameters [3÷6] $N \sim 2 \cdot 10^{19} c^{-1}$, $T \sim 1 \div 5$ eV, $6 = 10^3 \div 10^4$ 1/0m·m, a~0.1, a'~0.2 corresponding to criterion $\Pi = 20 \div 100$.

Laboratory measurements (see e.g. Ref.[5]) suggest that the electron temperature in the beam is practically constant ranging within $1 \div 10$ eV.

For this isothermal modes of plasma free expansion, the solution of the combined equations (6) of report [1] may be written as:

$$\frac{u^2}{u_0^2} = 1 + \frac{2}{\gamma M_0^2} \ln \frac{ua^2}{u_0 a_0^2} \; ; \qquad M_0^2 = \frac{m u_0^2}{\gamma T_0} \qquad\qquad 2.1$$

$$(a')^2 = (a'_0{}^2 + \frac{2C}{\gamma M_0^2} \ln \frac{a}{a_0}) \frac{u_0^2}{u^2} \; ; \qquad\qquad 2.2$$

$$T = T_0 \qquad\qquad 2.3$$

$$u/u_0 = (a/a_0)^{2-C} \qquad\qquad 2.4$$

$$fy = (1 + \eta^2)^{1+C/2} \qquad\qquad 2.5$$

$$y^2 = (1+\eta^2)^{-1} \; ; \; \tau = 1 \; ; \qquad\qquad 2.6$$

The separation condition 2.4 is consistent with equation of motion 2.1 if the following relationships are satisfied:

$$\frac{u^2}{u_0^2} - 1 = \frac{2T_0}{mu_0^2} \ln \frac{ua^2}{u_0 a_0^2} \approx \frac{T_0}{mu_0^2} \frac{C}{C-2} \ln \frac{u^2}{u_0^2} \approx \frac{C}{C-2} \frac{1}{\gamma M_0^2} \left( \frac{u^2}{u_0^2} - 1 \right)$$

Therefore the separation condition for variables x and $\eta$ is satisfied, if

$$C = \frac{2\gamma M_0^2}{\gamma M_0^2 - 1} \quad \text{and} \quad \frac{u^2}{u_0^2} - 1 \ll 1 \quad \text{or} \quad \left(\frac{a^2}{a_0^2}\right)^{2/\gamma M_0^2} - 1 \ll 1$$

Finally the following beam parameters distributions are obtained:

$$nu^2 = \frac{\dot{N} \cdot \nu \cdot u_c}{\pi a^2} \frac{1}{(1+r^2/a^2)^{\,p+1}} ;$$

$$\frac{u^2}{u_0^2} = (1+r^2/a^2)^{-1} ;$$

$$\frac{u_c^2}{u_0^2} = 1 + \frac{2}{\gamma M_0^2 - 1} \ln\left(\frac{a^2}{a_0^2}\right) \approx \left(\frac{a^2}{a_0^2}\right)^q ; \qquad\qquad 2.7$$

$$\nu = u\,(1 + a'^2 \cdot r^2/a^2) ;$$

$$(a')^2 = \left(a'^2_0 + \frac{2}{\gamma M_0^2 - 1} \ln\frac{a^2}{a_0^2}\right) \frac{u_0^2}{u^2} ;$$

$$n = \frac{\dot{N} \cdot \nu}{\pi a^2 \cdot u_c} (1+r^2/a^2)^{-p} ;$$

$$p = \gamma M^2/(\gamma M^2 - 1); \quad \nu = p - 1/2; \quad \gamma M_0^2 = \frac{mu_0^2}{T_0} ; \quad q = \frac{2}{\gamma M_0^2 - 1};$$

The initial part of SPT or TAL plume is characterized (see e.g. [4] ÷[7] ) with the following conditions:

$\gamma M_0^2 = mu_0^2/T_0 \sim 500 \div 100 \gg 1$, so that $u/u_0 = 1$ and $a' = a_0'$.

Resulting parameters distributions in conically expanding beam are the following:

- transverse size: $\qquad\qquad a^2 = x^2/k;$

- factor of flow divergency: $\qquad k = (a'_0)^{-2};$

- concentration: $\qquad\qquad n = \frac{\dot{N}}{2\pi u_c} \cdot \frac{k}{x^2(1+r^2/a^2)} ; \qquad 2.8$

- beam current density along axis x: $j_x = enu = \frac{e\dot{N}}{2\pi} \cdot \frac{k}{x^2(1+kr^2/a^2)^{3/2}} ;$

- impuls flux density along axis x: $mnu^2 = \frac{m\dot{N}u_c}{4\pi} \cdot \frac{k}{x^2(1+kr^2/a^2)^2} ;$

Transverse parameters distributions in isothermally expanding beam are more wide than that of adiabatically expanding jet so that peripherial energy amd substance fluxes in the beam are relatively greater.

## 2. Program and Calculation of Plasma free Expansion

### 2.1. General Description of Program

The dynamical problem solution, presented in report [1], is a mathematical base for development of PC program for calculation of plasma free expansion in space.

PC program DYNAMIC developed consists of two units JET and PLASMOID for calculation of flow characteristics of steady state and pulse plasma injections correspondingly.

The former calculates and plots:

- profile of plasma jet characteristic transverse size along the jet axis;

- radial dependencies of plasma concentration, temperature and velocity;

- lines of equal plasma concentration.

Input data are the particles flow rate and initial values of temperature, velocity, characteristic jet size and its derivative given at a plasma source exit.

Unit PLASMOID generally calculates three- dimensional plasmoid parameters for a time moment fixed resulting in:

- time profiles of three characteristic sizes of a plasmoid and three velocity- and temperature- components in the plasmoid center;

- time profile of plasma concentration in a given flow point;

- coordinate profiles of plasma concentration for a given moment;

- line of equal concentration in coordinate planes for given moment of time.

The input data are the total number of particles in a plasmoid, initial (t=0) values of characteristic sizes and their spatial derivatives, and also temperature given in the origin of coordinates.

Both units also accumulate data arrays in separate files to be further used for i.g. RF refraction / scattering calculations.

## 2.2. Representative samples of calculations.

Plasma expansion in space is determined by either the collision processes and initial conditions or inner self consistent electric fields. These fields arise due to high electron mobility and are proportional to local density and temperature gradients. In rarefied plasma the distribution of the inner fields is strongly influenced by the thermal conductivity of electrons providing effective transfer of energy to the periphery of plasma jet or cloud particularly from points of local energy releases. The ions are accelerated by inner plasma fields predominantly in the direction of the maximal gradient (across of a narrow jet or along the direction of heat flux). As a result the densities of energy and substance fluxes in expanding plasmas are sufficiently greater than in gases.

However these peripheral regions are extremely important since they determine the actual boundaries of arising inhomogeneities where the most practically interesting processes take place in fact. For instance namely these regions are essentially responsible for RF wave refraction/scattering and for electron collection by tether plasma contactors.
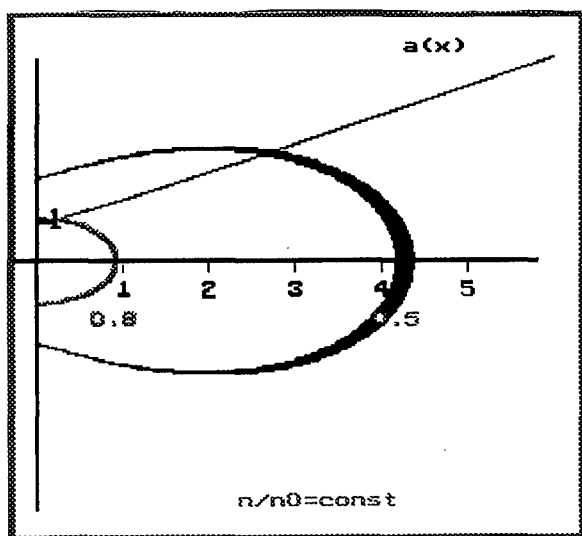
Fig.2.1 displays the results of calculation for free expansion of plasma plume of TSNIIMASH made experimental arcjet plasma source EPICURE. The procedure of input data determination based on laboratory measurements and more detailed comparison of the latters with theoretical issues

Fig.2.1

obtained, is presented in Sec.3 It is believed that the observed increase of curve a(x) inclination at low values of x represents the 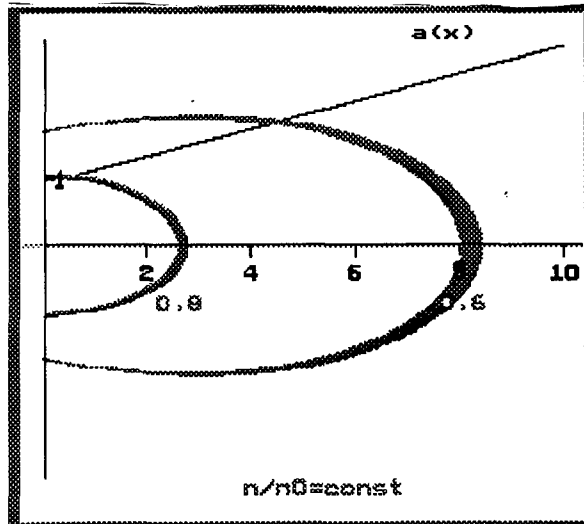adjacent to the source exit region of one - two exit orifice diameters long where energy exchange between plasma species still takes place before plasma becomes "frozen" and stream lines become straight.



Fig.2.2

Fig.2.2 illustrates jet expansion of very high Mach number (M=14) for highly focused charge compensated plasma beam.

The characteristic property of plasmoid three-dimensional expansion, namely the non-uniform increase of its sizes clearly seen in Fig.5 of Appendix A. If initial velocities are low compared to the mean random velocity, $v_T \sim \sqrt{T_0/m}$, the resulting velocity is maximal along the coordinate axis where the initial size of a plasmoid is minimal. Consequently resulting size of a plasmoid along this coordinate finally occurs to be maximal. So inversion of sizes takes place.

For example, a plasmoid initially generated as a "knitting needle" stretched along axis x, later transforms in a disk with minimal x dimension. In contrary a dense disk may transform in a long "knitting needle". The reason of this inversion is clear enough: the thermal energy initially accumulated by a plasmoid, gradually transforms in kinetic energy of expansion predominantly in the direction of maximal gradient of electric potential or in other words along the maximal gradient of total inner pressure $\nabla(nT_i + nT_e) \approx \nabla nT_i + en\nabla\Phi$ .

The results of calculations were further used for comparison with available data on Plasma free expansion.

# 3. Comparison of results obtained with available data on Plasma and Gas free Expansion

## 3.1. Comparison with Experimental Data In-House

Thorough measurements of plasma free expansion characteristics were undertaken in the plume of the experimental arcjet plasma source EPICURE developed to conduct space experiments on interaction between RF-signal and an electric thruster plume.

The device basic characteristics are:

- input power ....<2 kW (28V x 70A);
- propellant ............ caesium;
- total propellant load.... 0.3 kg;
- mass flow rate...... up to $30 \cdot 10^{-6}$ kg/s.

Two operating modes were chosen for comparison of experimental and theoretical data. The first one with discharge current of 35 A occurred to be corresponding to adiabatical flow with criterion $\Pi < 1$ and the second one of 65 A – corresponding to isothermal flow with criterion $\Pi > 1$.

The plasma plume basic characteristics – electron density, n , temperature, T , and Mach number, M, – were measured by Langmuir oriented cylindrical probes located along the vacuum chamber axis at the distances, R, of 0.3; 0.7; and 1.2 m from the plasma source nozzle exit orifice. Table 1 accumulates the plasma parameters measured at the flow axis, for two operating modes mentioned above.

Table 1

| operating mode | 35 A | | | 65 A | | |
|---|---|---|---|---|---|---|
| distance, R, m | 0.3 | 0.7 | 1.2 | 0.3 | 0.7 | 1.2 |
| density, n, $cm^{-3}$ | $6 \cdot 10^{11}$ | $10^{11}$ | $2.5 \cdot 10^{10}$ | $2 \cdot 10^{11}$ | $3 \cdot 10^{10}$ | $0.7 \cdot 10^{10}$ |
| temperature, T, eV | 0.3 | – | 0.26 | 1.8 | – | 1.6 |
| Mach number, M, | 2.5 | – | 2.6 | 2.5 | – | 2.6 |

The plasma source was mounted on a rotating gear to scan the plasma plume. Fig.3.2 shows the measured angular dimensionless profiles of $n(\Theta)/n_c$, where $n_c$ is the value of electron density at the flow axis. The profile at $R_3 = 1.2$ m where processes of energy exchange in the plume are believed to be over and the flow becomes conical, was used to determine the value of flow divergency factor, $k=(a'_0)^{-2}$, and particles flow rate, $\dot{N}$, via the self-similar angular distribution for the operating mode of 35 A:

$$n(\Theta) = \frac{\dot{N}\nu k}{\pi R_3^2 u_3} \cdot \frac{u_3}{u} \cdot \frac{1}{(1+k \cdot tg^2\Theta)^p}$$

$$\frac{u_3^2}{u^2} = 1 + \frac{2}{(\gamma-1)M_3^2} [1-(a_3/a)^q]$$

$$p = \gamma M^2/(M^2-1); \quad \nu = p-1/2 \;; \quad q = \frac{(\gamma-1)M^2}{M^2 - 1}$$

and expression

$$n_c = n_3(R_3, 0) = \dot{N}\nu k/\pi R_3^2 u_3.$$

The numerical values of k and $\dot{N}$ are equal 3.0 and $3.4 \cdot 10^{19}$ 1/c correspondingly so that the criterion $\Pi$ is equal 0.2, e.i. the flow is an adiabatical one ($\Pi < 1$).

These numerical values of k and N were used as the input data for PC program DYNAMIC to calculate the profile of plasma jet characteristic transverse size, $a(x)$ along the jet axis. This calculated profile $a(x)$ is plotted in Fig.3.1 with added three experimental points revealing good agreement.

The dependence $a(x)$ was used to calculate self-similar angular distributions according to relationships

$$\frac{n}{n_c} = \frac{a_c^2}{a^2} \cdot \frac{u_c}{u} \left(1 + \frac{R^2 \sin^2\Theta}{a^2}\right)^{-p}$$

$$\frac{u^2}{u_c^2} = 1 + \frac{2}{M^2(\gamma-1)} \left[1 - \left(\frac{a_c^2}{a^2}\right)^q\right]$$

Here $n=n(R,\Theta)$, $n_c=n(R,0)$, $a_c=a(R,0)$, $a=a(R \cdot \cos\Theta)$.

The calculated electron density distributions are compared

with experimental ones in Fig.3.2 for three distances R=0.3, 0.7 and 1.2m from the nozzle exit orifice.

Fig.3.2 suggests that there is a good agreement between theory and experiment for R=0.7 and 1.2m. Comparison of theoretical and experimental distribution at R=0.3m is not correct since the ionization processes are not still over within this nearest downstream region. This suggestion is confirmed by spectroscopic measurements.

The Robert's approximation (see Ref. [2] from report [1]) are also plotted in Fig.3.2 revealing agreement with the experimental data only within the core of the flow.

For the operating mode of 65A the numerical values of k and N are found to be 5 and $4.2 \cdot 10^{19} 1/c$ correspondingly so that the criterion $\Pi$ is of about 4, e.i. the flow is actually an isothermal one ($\Pi > 1$).
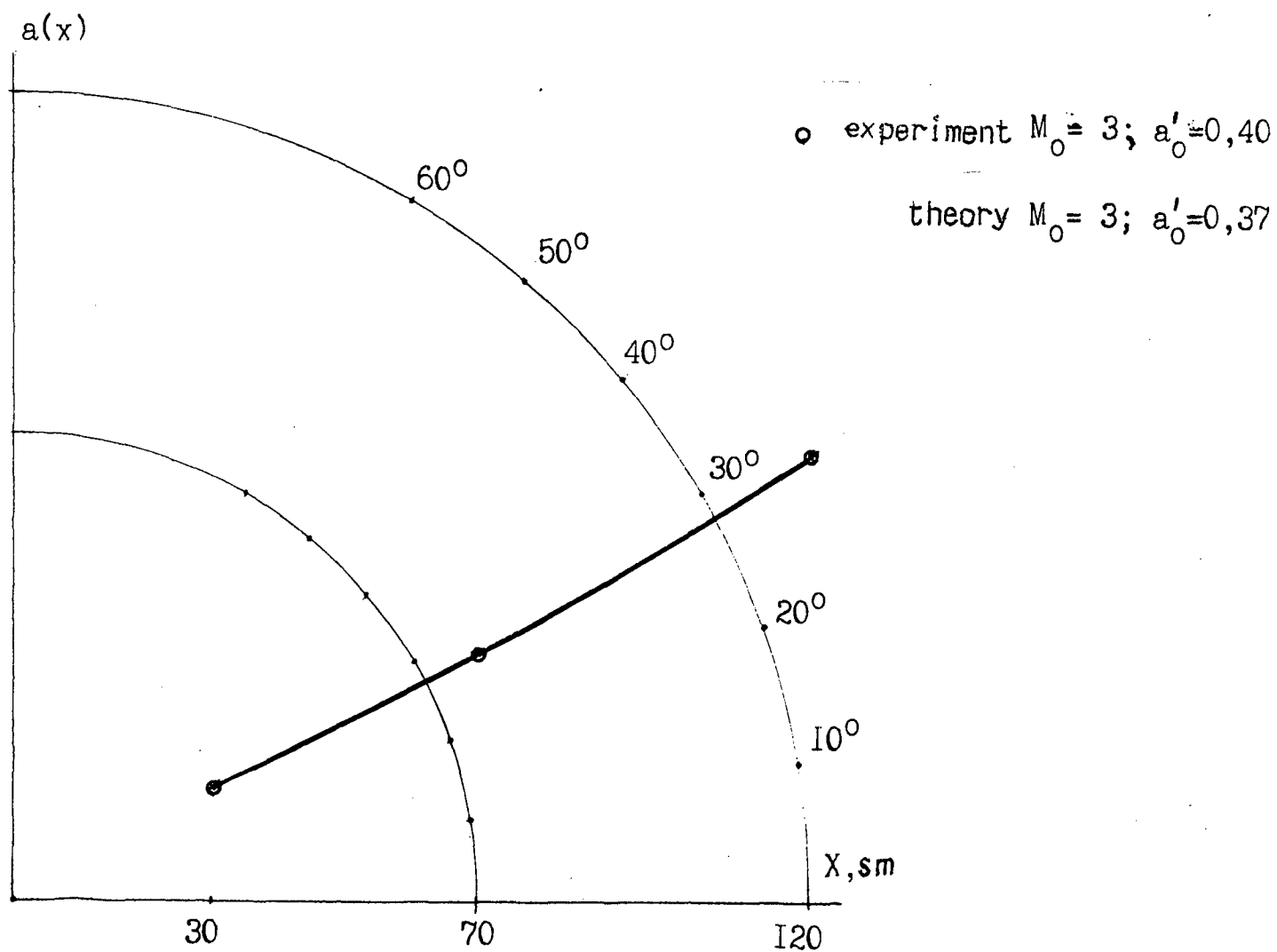
Using the same procedure to determine the dependence a(x) (see Fig. 3.3) again the self-similar angular density distribution was calculated according to relationships

$$\frac{n}{n_c} = \frac{a_c^2}{a^2} \cdot \frac{u_c}{u} \left(1 + \frac{R^2 \sin^2\theta}{a^2}\right)^{-p}$$

$$\frac{u^2}{u_c^2} = 1 + \frac{4}{\gamma M_0^2 - 1} \ln\left(\frac{a}{a_0}\right)$$

The resulting curves are compared with experimental electron density distributions in Fig.3.4 for three distances R=0.3, 0.7 and 1.2m from the nozzle exit orifice also revealing better agreement in the far region of the flow field.

Comparison of the theory and experiment presented above, confirms that the mathematical model of plasma free expansion correctly describes not only conical flow with ultimate velocity and straight flow lines in far region but also in adjacent to nozzle flow region where plasma heat energy accelerate the flow and flow lines diverge.

a(x)

60°
50°
40°
30°
20°
10°

o  experiment $M_0 \doteq 3$; $a_0' \doteq 0,40$

theory $M_0 = 3$; $a_0' \doteq 0,37$

X, sm

30        70        I20

3.1 Adiabatical plume expansion
   for Epicure arcjet ($\Pi < 1$)

experiment

⊙ R = 30 cm

△ R = 70 cm

▣ R = 120 cm

self similar model

—— R = 70 cm

--- R = 120 cm

Roberts model

—·— R = 120 cm

discharge mode:

$V_a$ = 26÷28 B

$I_a$ = 30÷35 A

$n_e / n_{ec}$

1,0

0,75

0,5

0,25

0    20°    40°    60°    80°
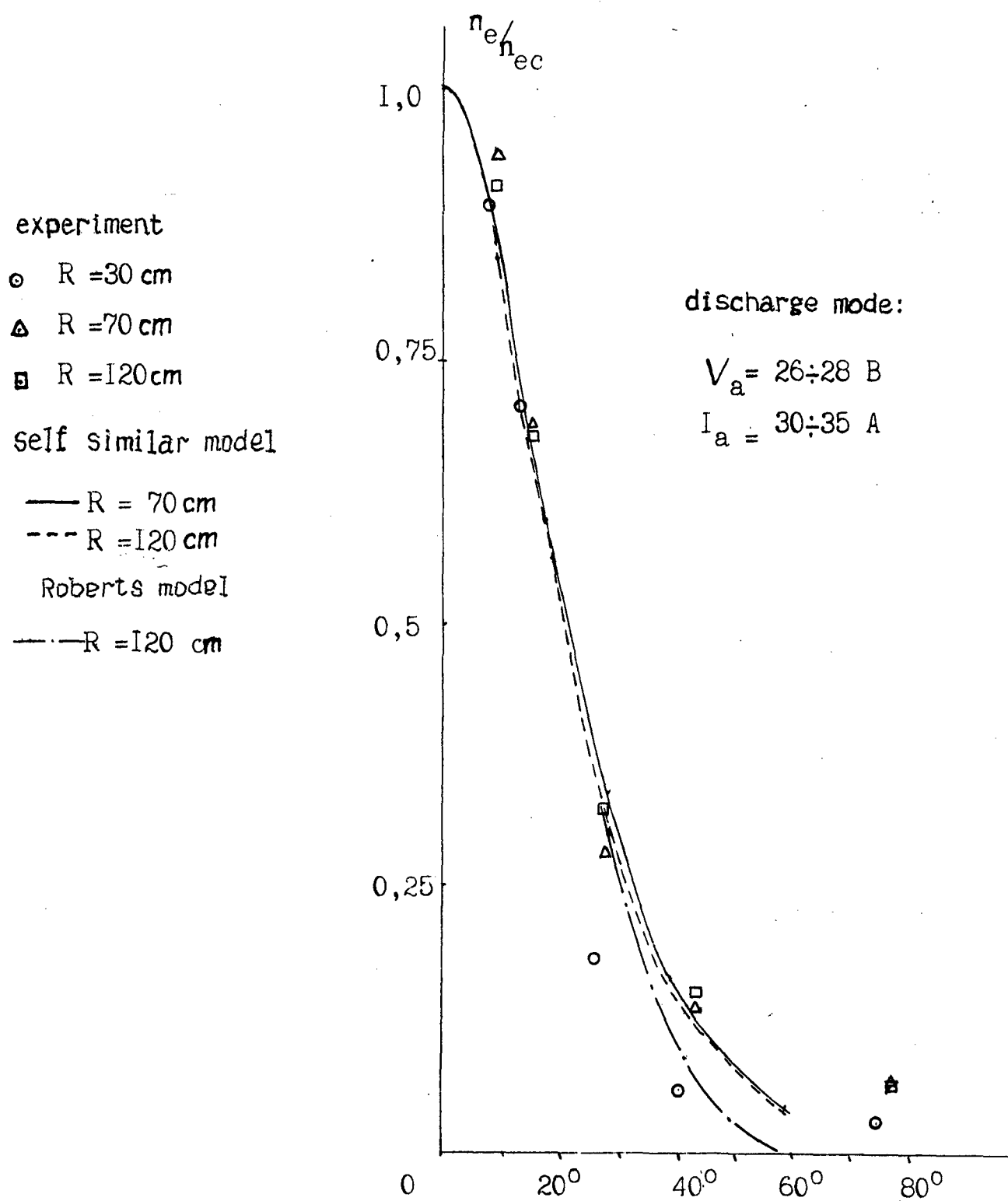
3.2 Transversal density distribution
in adiabaticaly expanding plume
of Epicure arcjet   ( Π < 1 )

o experiment $(M_O \approx 2,5; a_O' \approx 0,35)$

a(x)

60°

50°

40°

30°

20°

10°

X, cm

0

30

70

I20
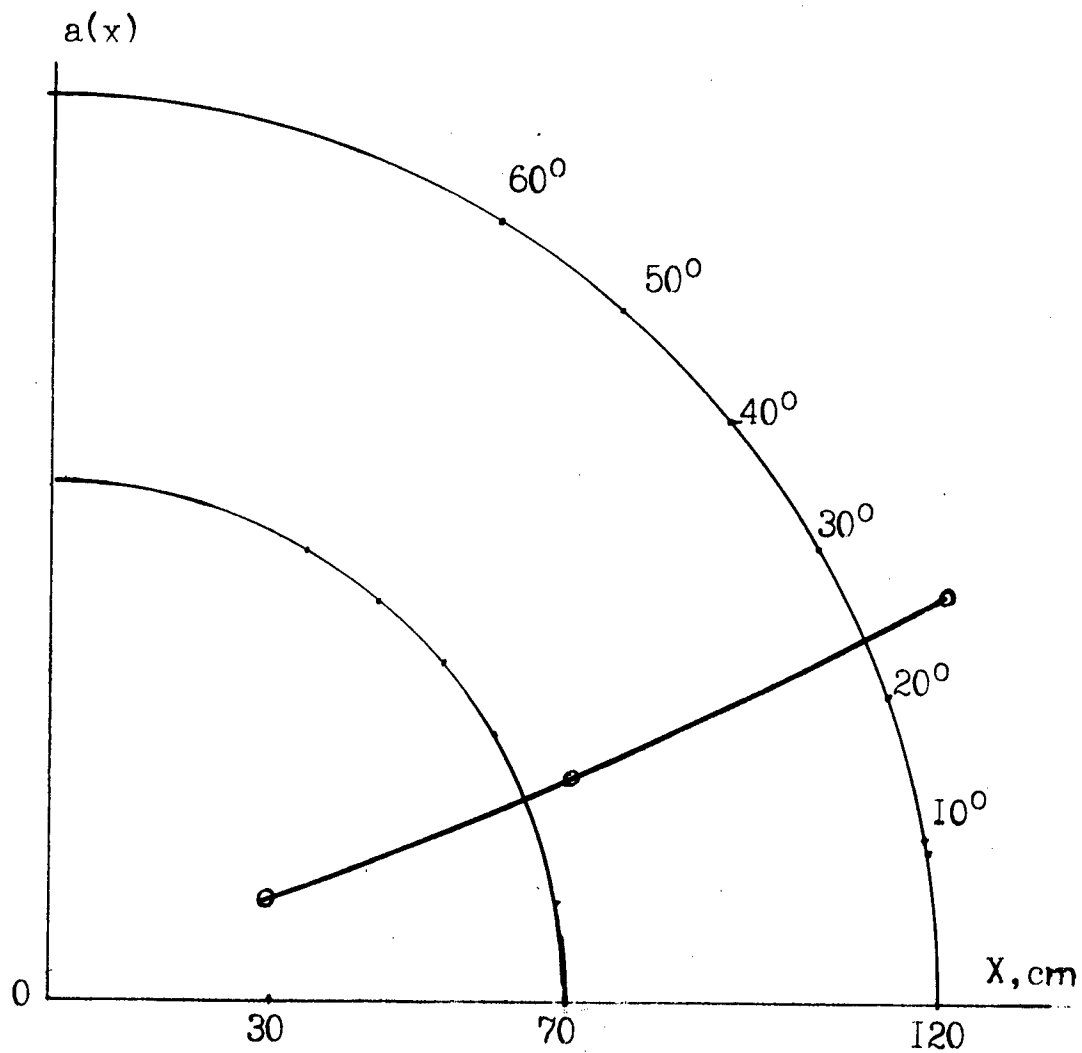
3.3 Isothermal plume expansion
for Epicure arcjet ($\Pi > 1$)

$^n e/n_{ec}$

experiment   theory  (P = I,I)

R = 30cm  •
R = 70cm  ×    ———
R =120cm  ○    —·—

discharge mode:

$V_a$ =27 B    $I_a$ = 65 A
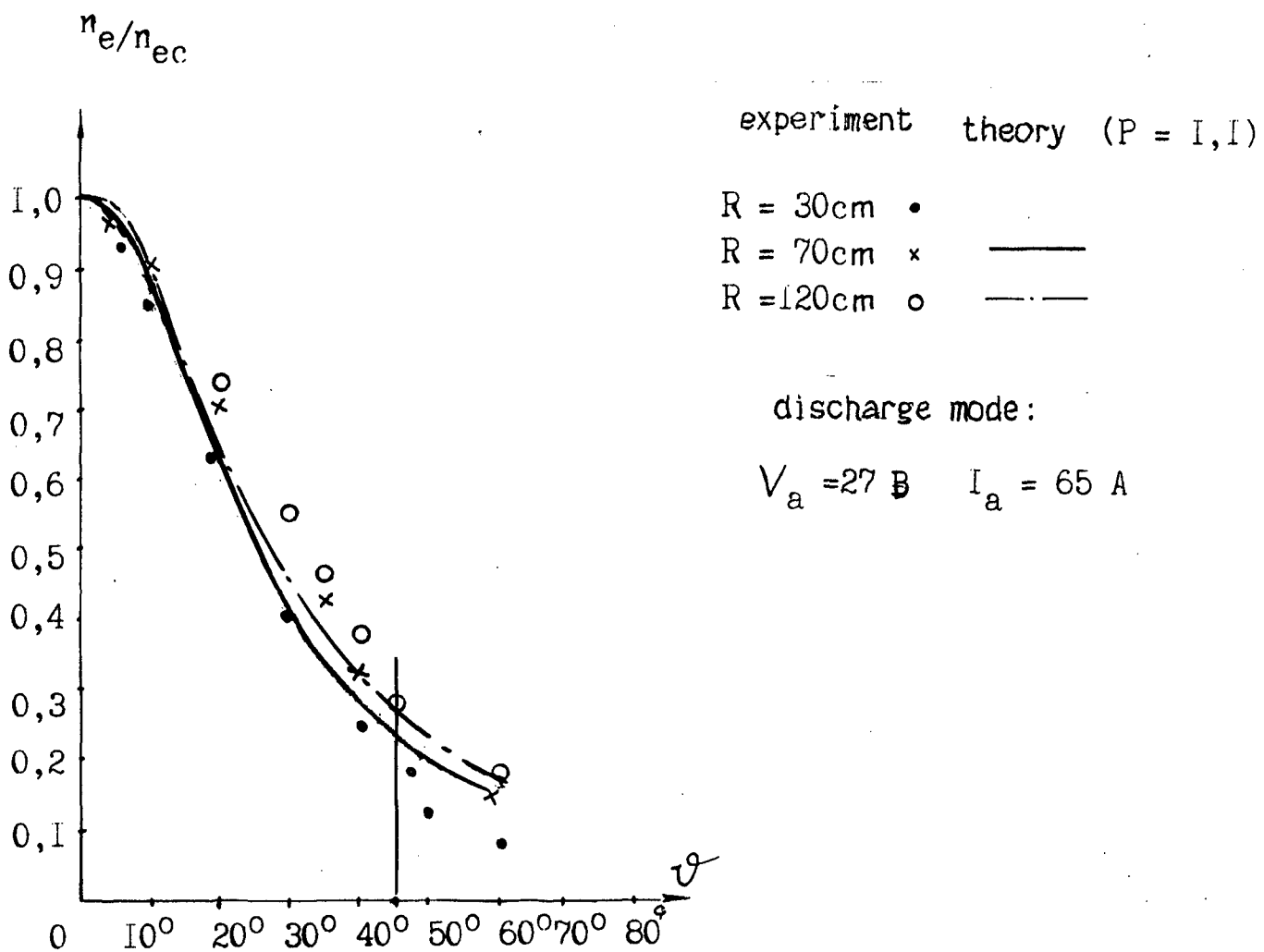
3.4 Transversal density distribution
    for the isothermal mode of expansion
    of Epicure arcjet plume ( Π > 1 )

## 3.2. Comparison with published results
### 3.2.1. Traditional thrusters

Ref. 3 concerns distributions of gas density, $\rho$, and substance and impulse fluxes, $\rho V$ and $\rho V^2$, in Simulate RSC plumes. Measured and calculated data are presented as angular dependencies in polar coordinates with the origin at the center of the nozzle exit orifice. The measurements were made at relatively large constant distance R from the nozzle.

Comparison of the measurements with calculated data, based on certain mathematical models of gas flow, suggests that experimental angular distributions of gas density and substance and impulse fluxes are more sharp in the vicinity of flow axis and more soft at the periphery of that than calculated ones.

In the self-similar solution for adiabatically expanding jet the transverse distributions of the velocity head, $\rho V^2$, does not depend on angular distribution of $T(\theta)$ and $V(\theta)$. In polar coordinates system the velocity head distribution is written as

$$\rho V^2 = \frac{m\tilde{N}u_m \nu k}{\pi R^2} \cdot \frac{u_c}{u_m} \cdot \frac{(1+tg^2\theta)^2}{(1+ktg^2\theta)^{1+p}} ;$$

$$\frac{u_c^2}{u_m^2} = 1 + b \cdot [\ 1 - (1 + tg^2\theta)^q\ ] ;$$

$$p = \frac{\gamma M_m^2}{M_m^2 - 1} ; \qquad q = \frac{M_m^2(\gamma-1)}{M_m^2 - 1} ; \qquad b = \frac{2}{M_m^2(\gamma-1)} ;$$

Here $u_m$ and $M_m$ are maximal velocity and Mach number at the flow axis, $\theta = 0$.

It is taken into account that

$$a^2 \approx x^2/k = R^2\cos^2\theta/k$$

The self-similar distributions plotted in Figs. 3 and 5 from Ref.3 are given by

$$\frac{\rho V^2}{\rho_c V_c^2} = \frac{(1+tg^2\theta)^2 \cdot \{1+b[1-(1+tg^2\theta)^q]\}^{1/2}}{(1 + ktg^2\theta)^{1+p}}$$

Using function $f_1$ given by

$$f_1(\theta) = \left[\frac{\rho_c V_c^2}{\rho V^2}(1+tg^2\theta)^2 \cdot \frac{u_c}{u_m}\right]^{1/(1+p)} = 1 + ktg^2\theta$$
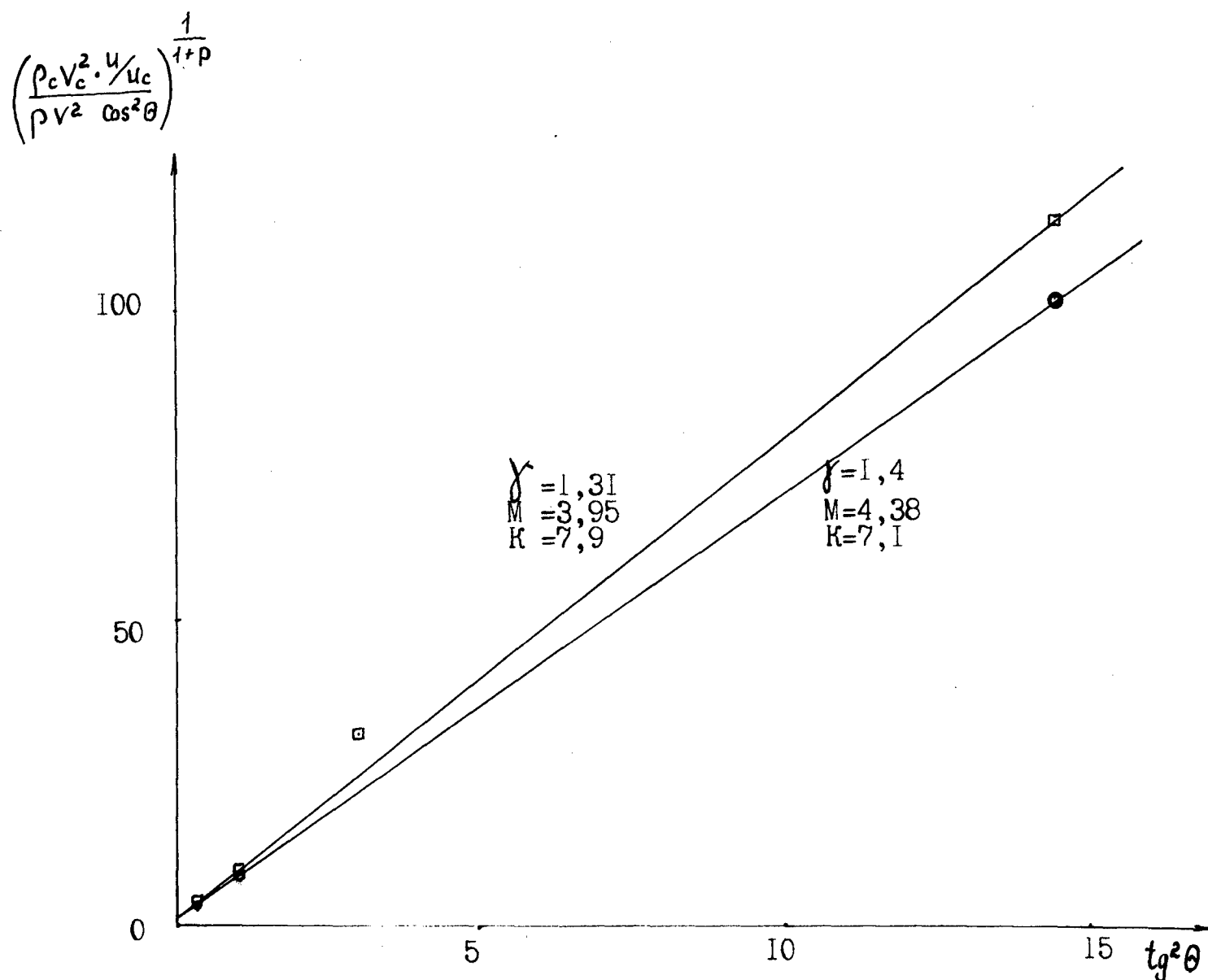
the measured angular dependence of $\rho V^2$ can be replotted so that the inclination of resultant straight line gives the value of flow divergency factor, k.

Fig.3.5 displays plots of function $f_1(\theta)$ for $N_2$ ($\gamma=1.4$) and mixture $N_2O_4$/A-50 ($\gamma=1.31$) providing values k=7.9 and k=7.1 correspondingly. For these two working substances Fig 3.6 and 3.7 show derived from Ref. 3 theoretical dependencies $\rho V^2/\rho_c V_c^2$ using the same coordinates.
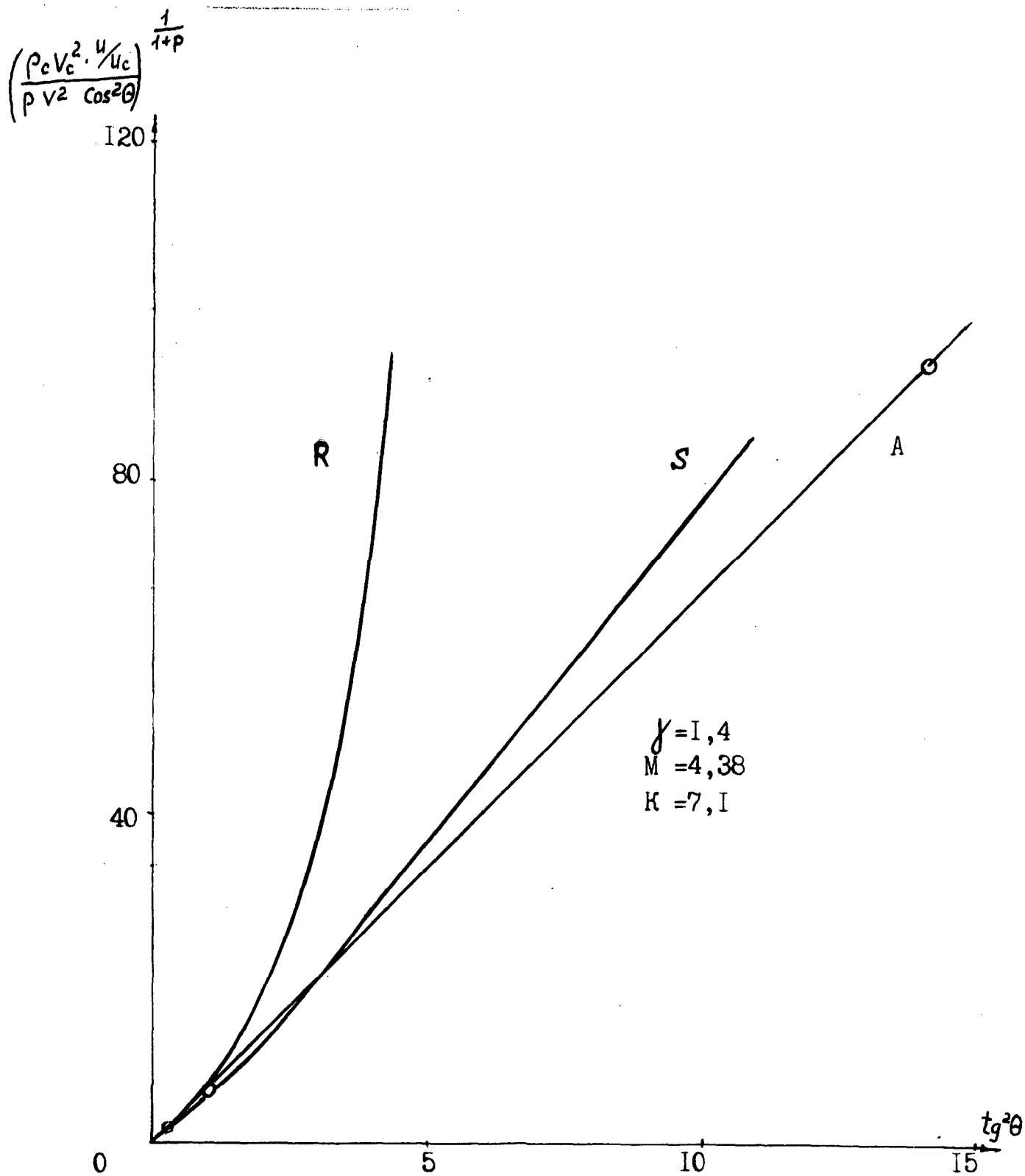
In Fig 3.8 the self-similar angular distributions are added to those derived from Ref[3] with corresponding values of Mach number. The curves of $\rho V$ and $\rho$ are obtained from self-similar angular distribution ($\rho V^2$) using experimental dependence $V(\theta)$ of Fig 2 from Ref. [3].

It is seen that the self-similar angular dependencies, displayed in Fig 3.6, 3.7 and 3.8 more accurately follow the experimental distribution of flow parameters than simple Robert's approximation or even more tedious numerical methods generally used. Particularly, the self-similar angular dependencies of all fluxes are more sharp in the vicinity of flow axis, $\theta < 45°$, and more soft at its periphery, $\theta > 60°$, than those calculated using other flow models of freely expanding gas. This is general difference between experimental and numerical results discribed in [3].

Really, the expression ($\rho V^2$) suggests that in the vicinity of flow axis, $20°<\theta<45°$, e.i. $1/k < tg^2\theta <1$, the order of magnitude for $\rho V^2$ is given by $\rho V^2 \sim (ktg^2\theta)^{-(p+1)}$ whereas at flow periphery, where $\theta > 60°$ and $tg^2\theta \gg 1$, the angular dependence of $\rho V^2$ is more soft: $\rho V^2 \sim k^{-(p+1)} \cdot tg^2\theta^{-(p-1)}$.

$$\left(\frac{\rho_c V_c^2 \cdot u/u_c}{\rho V^2 \cos^2\theta}\right)^{\frac{1}{1+p}}$$



$\gamma = 1,31$
$M = 3,95$
$K = 7,9$

$\gamma = 1,4$
$M = 4,38$
$K = 7,1$

$tg^2\theta$

3.5 Experimental data for $N_2$ and $N_2O_4$/A-50 plumes
from Ref. [3] plotted in special coordinates
to determine flow divergence factor according
to self-similar flow model

$$\left( \frac{\rho_c V_c^2 \cdot {}^{4}\!/\!u_c}{\rho \, V^2 \, Cos^2\theta} \right)^{\frac{1}{1+P}}$$

R

S

A

$\gamma = 1,4$
$M = 4,38$
$K = 7,1$

$tg^2\theta$

3.6 Experimental and theoretical data for $N_2$ plume
from Ref.[3] plotted in special coordinates
in comparison with self-similar flow model
R – Roberts' approximation
S – Simons' model
A – Self-similar model

Y-axis label: $\left(\dfrac{\rho_c V_c^2 \cdot u/u_c}{\rho V^2 \cos^2\theta}\right)^{\frac{1}{1+P}}$

X-axis label: $tg^2\theta$

Curve labels: V.T, V.L, S, A, Inv, R

$\gamma = 1,31$
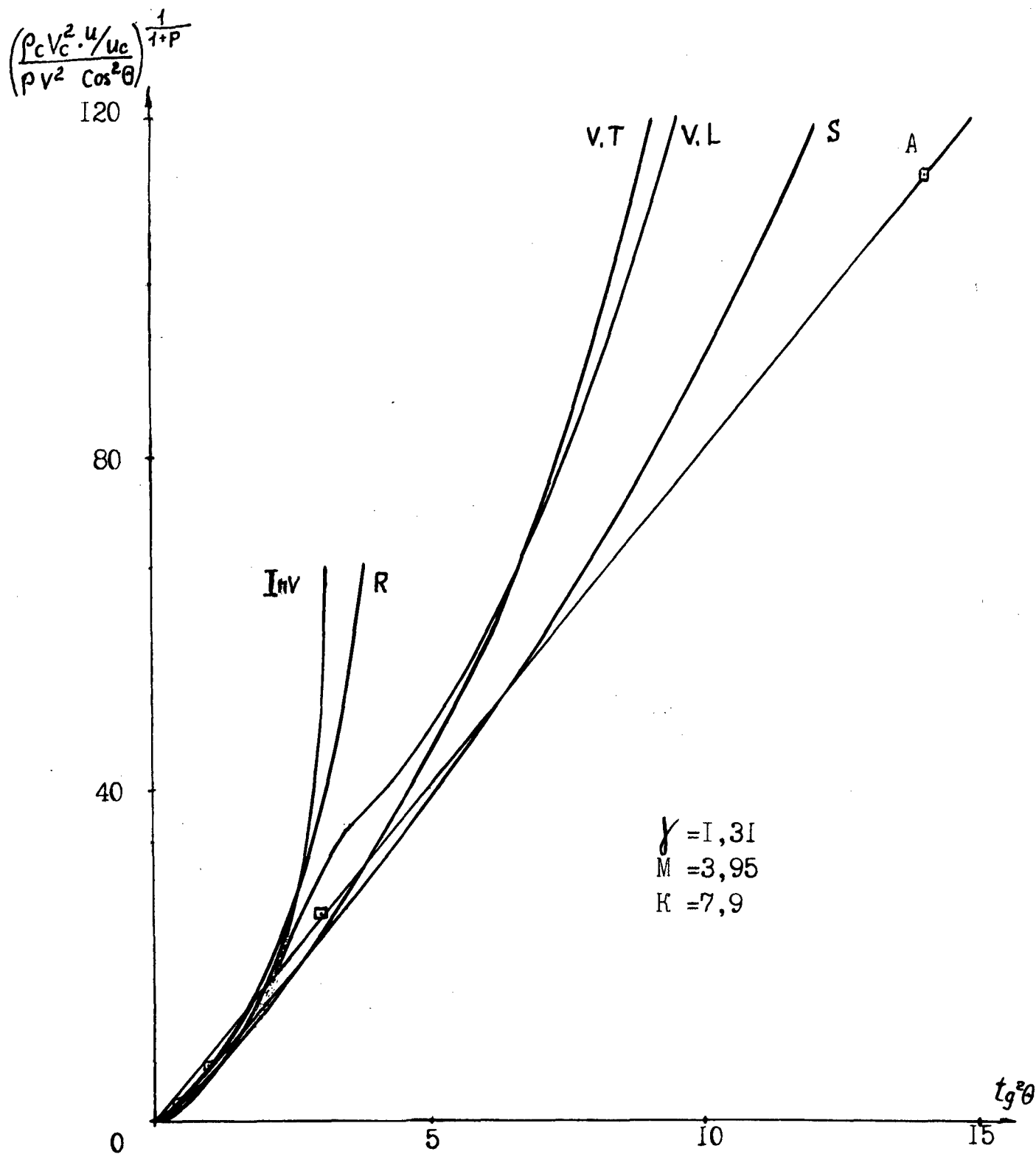$M = 3,95$
$K = 7,9$

3.7 Experimental and theoretical data for $N_2O_4$/A-50
   plume from Ref. [3] plotted in special coordinates
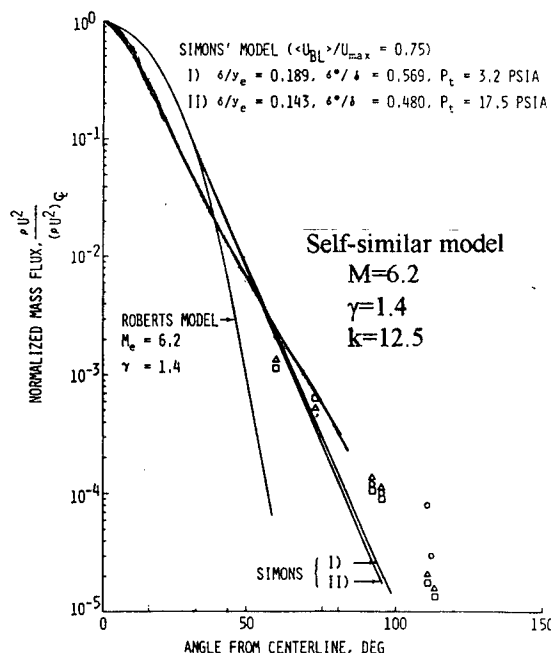   in comparison with self-similar flow model
        R − Roberts' approximation
        S − Simons' model
        A − Self-similar model
      Inv − Inviscid
    VT.VL − Viscid turbulent and laminar

**Fig. 2** Normalized mass flux and velocity measurements in the plume of a 1/10-scale Lunar Module RCS engine.



**Fig. 4** Comparison of measured density ratio with predictions from Simons' model.



**Fig. 3** Comparison of measured dynamic pressure profile with Boynton's predictions.



**Fig. 5** Comparison of Chirivella's measured flux ratios with predicted density ratio from Simons' model.

3.8  Experimental and theoretical plots of Ref. [3]
     with self-similar curves added for comparison

## 3.2.2. Electric Thrusters Plumes

Operation of onboard Stationary plasma (SPT) or Anode layer (TAL) electric thrusters results in arising in space of expanding ion beam with the following representative initial parameters :

ion energy $\qquad E_0 = mv_m^2/2 = 270$ eV;

electron temperature $\qquad T \sim 1 \div 5$ eV;

values of square Mach number $\quad M^2 \sim mv_0^2/T_0\gamma \approx 300 \div 60$;

corresponding to criterion $\quad \Pi = 6T_e\pi aa'/e^2\dot{N} \sim 20 \div 1000$.

Consequently ion beam expansion is isothermal under the condition of $M^2 \to \infty$.

Taking into account that for the nearest flow region

$$a_0'^2 = \text{const} = 1/k, \quad \text{for} \quad a/a_0 \ll \exp(mv_0^2/2T_0)$$

we obtain conical beam expansion.

Ref. 4 presents the distribution of ion beam current density $j(x,r)$ measured in cylindrical coordinates. There is a self-similar relationship for this quantity:

$$j_x = \frac{e\dot{N}k}{2\pi x^2} \cdot \frac{1}{(1+kr^2/x^2)^{3/2}} \quad ;$$

Theoretical and experimental dependencies can be compared using two independent methods. The ion beam current density at the axis is expressed via total ion beam current, $I_i = e\dot{N}$, and factor of flow divergency, k.

$$j_c = \frac{e\dot{N}k}{2\pi x^2}$$

The measured transverse dependence of $j_x$ can be replotted in the special coordinates

$$f_2(\eta^2) = (j_c/j_x)^{2/3} = 1 + k \cdot r^2/x^2$$

so that the inclination of resultant straight line gives the value of flow divergency factor, k.

Function $f_2$ is plotted in Fig. 3.9 for a few transverse secti-

ons of the ion beam for x ranging from 0.52 to 3.7 m. Fig.3.9 displays $j_c$(x) curve calculated for k =9.5 and experimental points for axial values of $j_c$. Experimental and calculated lines of equal values of $j_x$ are plotted in Fig.3.9.
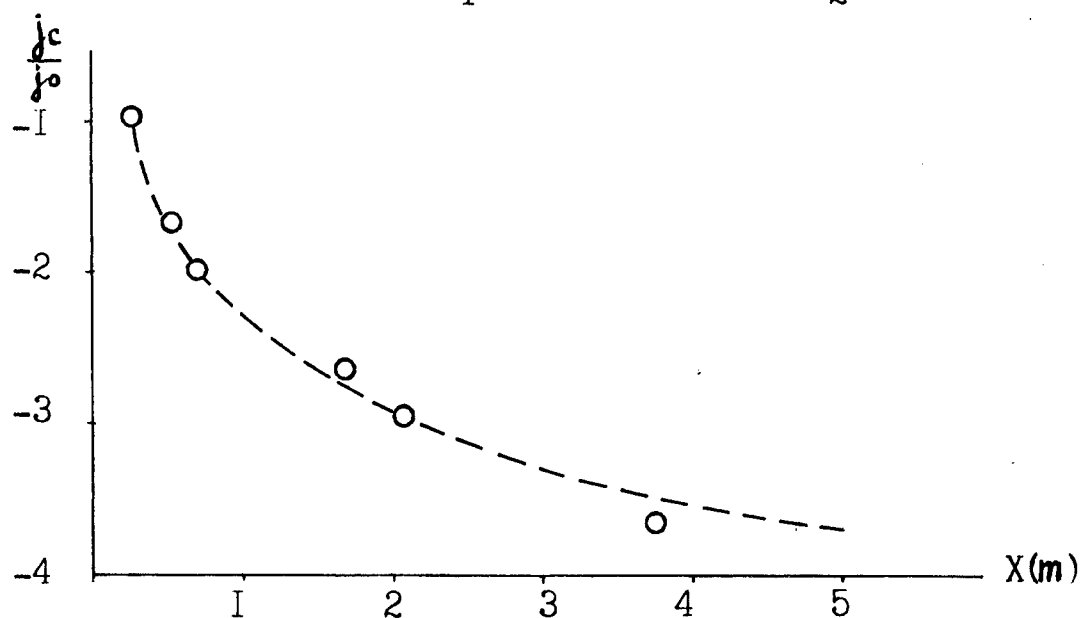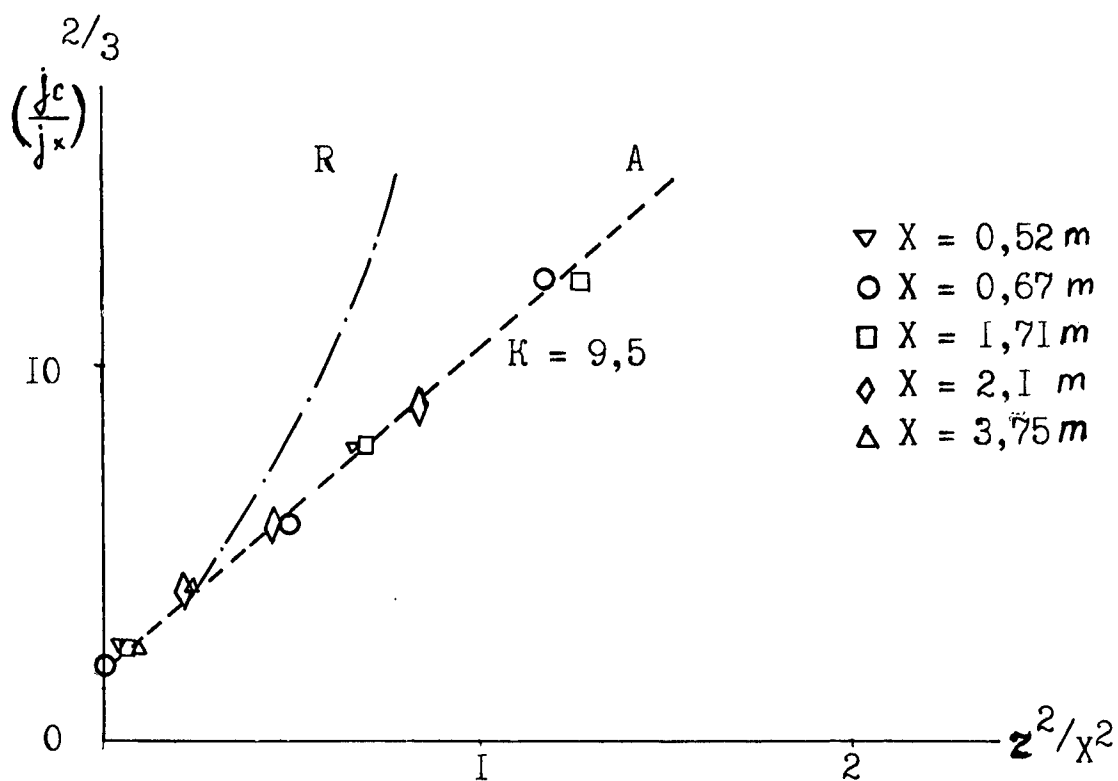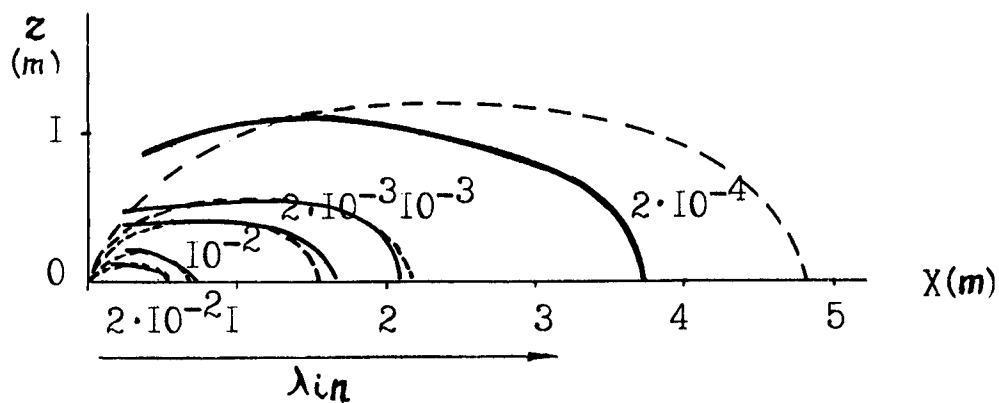
All three Figures suggest that experimental and calculated data satisfactorily correlate for x < 3 m. Under the conditions on ambient pressure for experiments of Ref. 4, the charge exchange free path length for $Xe^+$ ions is evaluated on the level of about 3m. Therefore the observed difference between experimental and calculated data for x > 3 m, is believed to be due to ion beam scattering in the ambient gas.

In Ref.[5] the angular distributions of ion beam current density, $j(\Theta)$, and ion energy, $E(\Theta)$, for SPT-70 electric thruster plume are measured in polar coordinates at constant distance R, from the exit orifice plane. The self-similar solution gives the following angular dependencies for these quantities:

$$env^2 \equiv j \cdot \sqrt{E/2m} = \frac{e\dot{N}k \cdot \sqrt{E/2m}}{2\pi R^2} \cdot \frac{(1+tg^2\Theta)^2}{(1+ktg^2\Theta)^2};$$

Again the appropriate function f3 can be plotted in the special coordinates so that the inclination of resultant straight line gives the value of flow divergency factor, k. From Fig.3.10 the resultant value of k = 9.6, practically is equal to that, k = 9.5, determined for another SPT version of the same design [4]. Although in Refs. 4 and 5 the SPT electric thrusters of the same design were studied, the measuring methods were principally different and vacuum facility conditions also differed. Coincidence of laboratory measurements processing results for these different cases suggests that the used analytical method is correct enough.

Let us compare the experimental data on ion beam expansion reported in Refs.6,7 and 8 for SPT-100 and TAL D-55 electric thrusters

$z$ (m)

I

$2 \cdot 10^{-3}$  $10^{-3}$  $2 \cdot 10^{-4}$

$10^{-2}$

0

$2 \cdot 10^{-2}$ I  2  3  4  5  X(m)

$\lambda_{in}$

$2/3$

$\left(\dfrac{j_c}{j_x}\right)$

R  A

$K = 9,5$

10

$\triangledown$ X = 0,52 m
$\bigcirc$ X = 0,67 m
$\square$ X = 1,71 m
$\diamond$ X = 2,1 m
$\triangle$ X = 3,75 m

0  I  2  $z^2/x^2$

$\dfrac{j_c}{j_0}$

-I

-2

-3

-4  I  2  3  4  5  X(m)

3.9 Comparison of experimental data from Ref. [4]
for the SPT type electric thruster exhaust
beam with the self-similar flow model of
isothermal expansion mode
— — — — — — self-similar model
— · — · — · — Robert's approximation

$$\left(\frac{j_c}{j \cdot \cos^3\theta}\right)^{3/2}$$

$$\left(\frac{j_c\sqrt{E_c}}{j\sqrt{E} \cdot \cos^4\theta}\right)^{1/2}$$

K=26

K=9,6

$tg^2\theta$
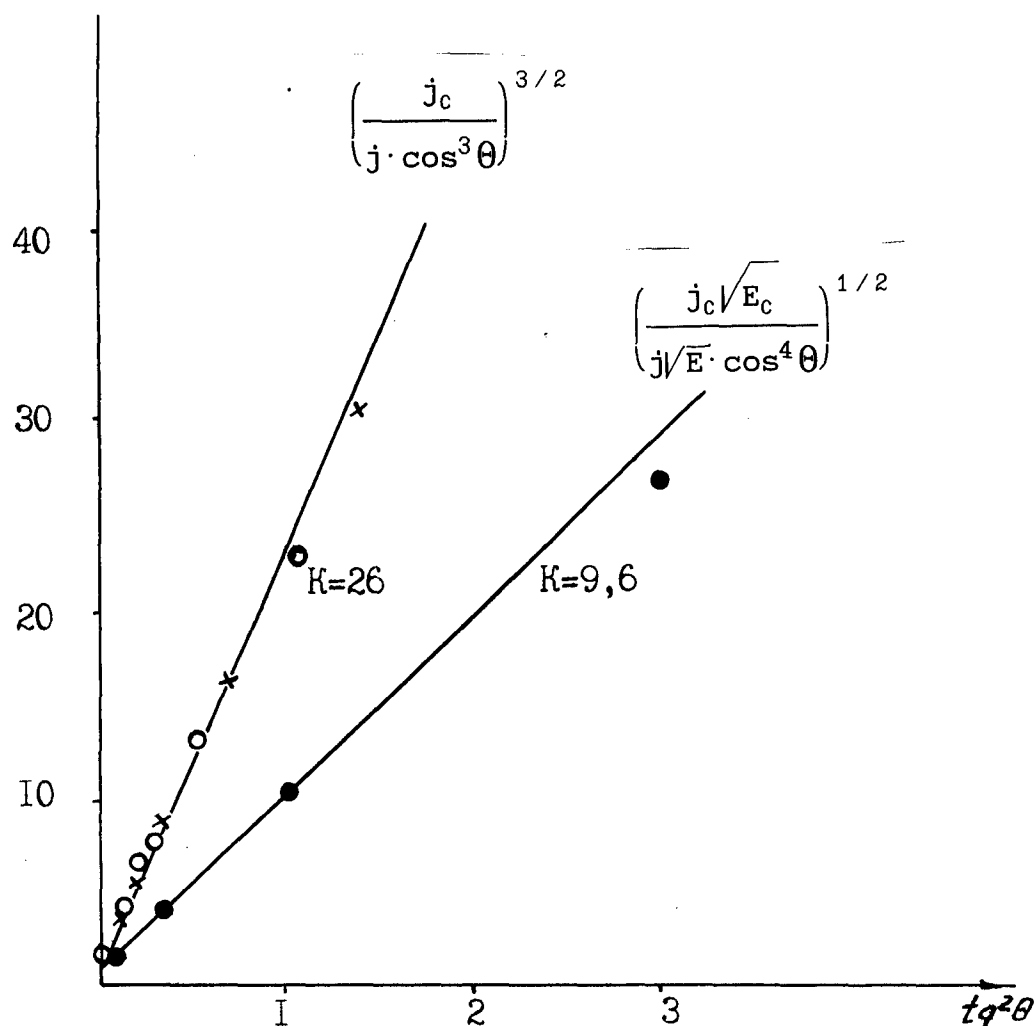
3.10 Comparison of experimental data from Ref.[5-8]
for SPT-70, SPT-100 and TAL D-55 electric engines
plumes with the self-similar flow model of
isothermal expansion mode

•　　　　　SPT-70 experiment [5]

o　　　　　SPT-100 experiment [6,7]

x　　　　　TAL D-55 experiment [6,8]

─────────　self-similar model

of different design under the conditions of the same operating mode: accelerating voltage of 300 V, discharge current of 4.5 A and equal Xe mass flow rate. Value of electron temperature, $T_e$, is arbitrary taken at its upper limit of 5 eV.

Self-similar ion beam current density is given by;

$$J_i = env = \frac{e\hat{N} \cdot k}{2\pi R^2 \cos^3 \theta} \cdot \frac{1}{(1+k tg^2 \theta)^{3/2}};$$

Again the appropriate function $f_4$ being plotted in the special coordinates, gives the value of flow divergency factor, k. Fig.3.10 shows that the resultant values of k occur to be equal 26 both. This suggests that two ion accelerators using almost the same physical principles despite of different design, provides practically the same beam focusing with characteristic divergence

$$arctg(a') = 11^0$$

It is also shown that plumes of Stationary plasma (SPT) or Anode layer (TAL) electric thrusters producing high velocity ion beam, are characterized with more spread substance fluxes than gas flows due to action of radial electric fields produced by the electronic specie.

# Discussion

The demonstrated above good agreement between experimental and theoretical data suggests that here presented approach to formulation and solution of plasma free expansion dynamical problem is fruitful and correct enough.

This approach can be further developed to evaluate interaction of freely expanding plasma with environment both in vacuum facifities and space.

In Ref. [7] was noted that lowering of background pressure in vacuum chamber results in electric thruster plume increase in contradiction to predictions based on mechanisms of beam scattering in residual atmosphere. It means that electric thruster exhaust beam divergence in deep vacuum of space flight may be significantly greater than that on-ground measured.

Authors of Ref. [9] attempted to explain temporal degradation of SPT operating characteristics, taking into account processes of plume interaction with ambient gas and subsequent impact to accelerating mechanisms in SPT.

The described above method of plasma jet parameters calculation also may be used to study the mechanisms of plasma jet interaction with ambient gas resulting in correction of on-ground measured parameters of electric thrusters for the actual conditions of space environment. Particularly, the unexpected results of Ref. [7] may be satisfactorily explained.

This approach also allow to evaluate the expected impact of the spacecraft ambient atmosphere including return fluxes of substance released.

The formulation and solution of dynamical problem on plasma free expansion presented in Report [1], may be readily updated to

take into account electric currents flowing in plasma and ambient media, e.g. in metallic walls of vacuum chambers and in ionosphere. The former updating could be further used to improve correctness of on-ground measurements and the latter one is perspective for development of theory of plasma contactors for electrodynamical tethers in space.

The solutions of plasma expansion problem obtained, are valid in relatively near region of plasma flow where forces of interaction of flowing plasma and magnetic field are low compared to pressure gradients.

The relation between these forces is determined by so called parameter of magnetic interaction,

$$S = \frac{6u^2 B^2 \pi a^3 a'}{\dot{N}T}$$

The characteristic size of plasma flow, where $S < 1$ and action of magnetic field is relatively insufficient is given by

$$X_B = \left(\frac{\dot{N}Tk^2}{6u^2 B^2}\right)^{1/3}$$

For example this estimated size for plume of Epicure arcjet (see Section 3.1), operating in space is of about 3,2 m with due regard for action of the Earth magnetic field. For plume of electric thruster of SPT type (see section 3.2.2) this size is only 2 m.

Therefore for many real situations the action of the Earth magnetic field must be taken into account while evaluating interaction of on-board devices plasma plumes with environment and spacecraft structure, and calculating RF scattering effects.

# Conclusion

The dynamical problem describing evolution of both fully ionized stationary supersonic plasma jet and plasmoid injected from a spacecraft is formulated and solved in a self-similar form.

Because of the self-similar approach and reasonable simplification the initial combined partial differential equations of two components plasma dynamics were rearranged in a set of separable equations so that the problem was reduced to quadratures and to solution of ordinary nonlinear differential equations.

Analytic forms of the solution were obtained for practically interesting ultimate thermal modes of plasma flows including
- hypersonic adiabatic plasma or gas jet expansion;
- isothermal expansion of highly accelerated ion beam and
- ellipsoidal plasmoid.

The dynamical problem solution obtained, properly describes either the adjacent to a nozzle region of non-linearly expanding flow or the far region of inertial expansion.

The most noticeable feature of three dimensional plasmoid expansion is the inversion of its shape.

Validity of theoretical result obtained is confirmed by the way of comparison with in-house experimental and/or published data. Good agreement between experimental and theoretical data is demonstrated for traditional and electric thrusters plumes both. It is also shown that presented mathematical model of freely expanding plasma jet more precisely follows the experimental data than Robert's and Narasimha's approximations often used.

The obtained dynamical problems solutions were put in the base of PC Program DYNAMIC developed to calculate characteristics of free expansion of artificial plasma formations in space. Compact forms of solutions used, result in great saving of run time. The Program DYNAMIC allows "to visualise" plasma flow field and provides data for numerous application including i.g. RF refraction / scattering calculations. necessary for determination of communication, navigation and ranging conditions for a spacecraft.

* * *

# References

1. Development of Dynamical and Mathematical Models of Exhaus-
   ted Plasma Plumes and Plasmoids in Space.
   Dynamical Problems Formulation and Solution.
   INTERMEDIATE REPORT EOARD Contract SPC-94-4081.
2. B.S.Borisov,     V.I.Garkusha,     N.V.Kozyrev,     A.G.Korzun,
   L.Yu.Sokolov,  V.A.  Strashinsky. The Influense of Elektric
   Thruster Plasma Plume on Downlink Communication in Space Ex-
   periments // AIAA 91-2349, 27th Joint Propulsion Confe ren-
   ce, June 24-26, 1991 / Sacramento, Ca. 11p.
3. Calia  V.S.  and  Brook J.W.,  "Measurements of a Simulated
   Rocket Exhaust Plume Near the Prandtl-Meyer  Limiting  Ang-
   le.",  J.  Spacecraft,  Vol.  12,  No.  4,  Apr.  1975, pp.
   205-208.
4. Askhabov S.N. et.al.," Investigation of the Plume of Stati-
   onary Plasma Thruster with Closed Electron  Drift",  Plasma
   Physics (in Russian), Vol. 7, No. 1, 1981, pp. 225-230.
5. Absalamov S.K.  et.al.  Measurement of Plasma Parameters in
   the  Stationary Plasma Thruster (SPT-100) Plume and its Ef-
   fect on Spacecraft Components.  /  28-th  Joint  Propulsion
   Conference and Exhibit. July 6-8,1992. Nashville, TN, Paper
   AIAA-92-3156.
6. D.H.Manzella,  J.M.Sankovic,"Hall Thruster Ion Beam Charac-
   terization", 31st JPCE by AIAA, ASME, SAE, and ASEE San Di-
   ego, California, July 10-12, 1995, AIAA-95-2927.
7. J.M.Sankovic,  T.W.Haag, D.H.Manzella, "Performance evalua-
   ·tion of a 4,5 kW SPT thruster", IEPC-95-30
8. A.V.Semenkin et.al., "Experimental study of exhaust beam of
   anode layer thruster", IEPC-95-51.
9. A.I.Bugrova, A.I.Morozov, "The influence of vacuum conditi-
   ons on SPT operating", IEPC-95-46.

# Program for calculation
# of plasma free expansion in vacuum
# DYNAMIC

## Program Description

### Content:

# 1.Assignment, content and conditions of use

1.1.Program DYNAMIC is intended to calculate characteristics of free expansion of artificial plasma formations (APF) arising in space due to operation of onboard plasma sources.

1.2. It consists of two units - JET and PLASMOID.

The former calculates characteristics of plasma jet free expansion in vacuum for plasma sources of steady state mode operation.

The latter calculates characteristics of plasmoid free expansion in vacuum for plasma sources of pulse mode operation.

1.3.Program DYNAMIC provides the following as a result of calculation:

-APF dimensional parameters;

-spatial and temporal distributions of plasma concentration and temperature;

-configuration of equal plasma concentration surfaces .

The Program presents the results of calculation run graphically on a display and also accumulates resultant data arrays in separate files of current directory for further use.

1.4. To put DYNAMIC run You need a IBM compatible computer with a keyboard of 101 keys and more than 100 kilobytes memory available in current directory.

1.5. Program DYNAMIC is developed in Turbo Pascal 7.0 integrated environment to be run with Microsoft MS DOS 6.2 or later version or compatible one.

Program DYNAMIC contains the following four files:

-DYNAMIC.EXE (the main file);

-STRM-IN (input data file of test example for JET unit);

-PLSD-IN (input data file of test example for PLASMOID unit);

-READ.ME (text file of user manual).

1.6.Program DYNAMIC provides the following:

-choice of calculation version;

-data entry, input data correction;

-calculation runs and resultant data soft copy;

1.7 The run time of one calculation version is of about 1 minute for RC AT 486.

## 2. How to run the Program

2.1. Getting Program DYNAMIC run is simple.  Insert DYNAMIC floppy disk  delivered in an appropriate drive or Enter the directory on hard disk where You have stored DYNAMIC files to save original floppy  disk and  choose  DYNAMIC.EXE.  resulting  in  appearance  of window 1 (see Fig.1) with brief description of Program DYNAMIC.
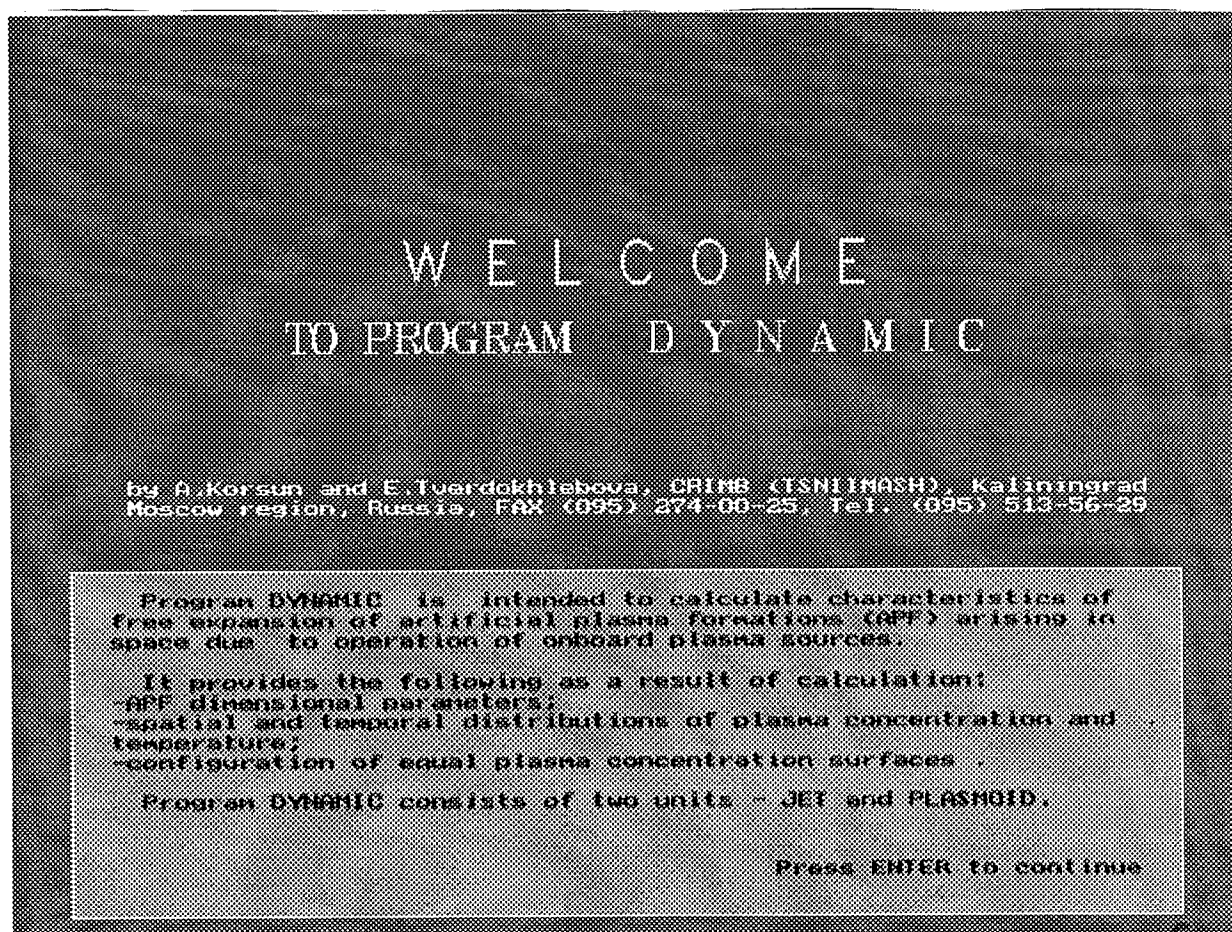


Fig.1

2.2. Press ENTER to display Program DYNAMIC MENU (see Fig.2). You can use the arrow keys to choose one of two Program units or press ESC to interrupt the Program run.

2.3. If You made Your choice,  press ENTER to open window 3  (see Fig.3 ).   In this window You can type new input data for  calculation pressing  ENTER  after each typing or choose ESC to start execution of the test example.  For more information about input  data  entry,  see descriptions of Program units.
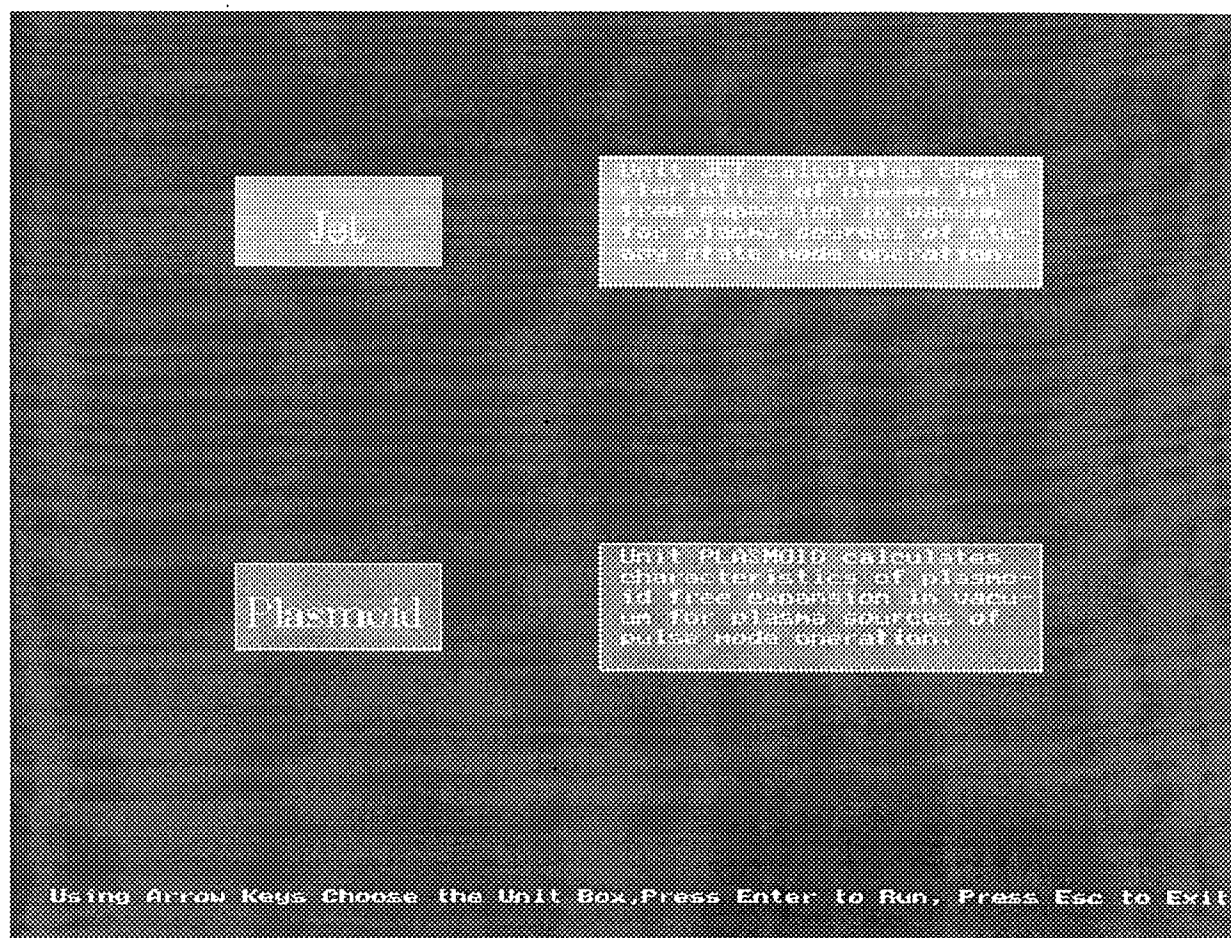
Fig.2

**Initial dimensionless parameters**



| Parameter | Identificator | Value limit | Test | New |
|---|---|---|---|---|
| Specific heat ratio | g | 1..5/3 | 1.666 | |
| Mach number | M | 2..15 | 2.5 | |
| Integration step | h | 0.001..1 | 0.01 | |
| Integration area | s | 1..100 | 8 | |
| Concentration order 1 | n/n0 | 0.99..0.01 | 0.8 | |
| Concentration order 2 | n/n0 | 0.99..0.01 | 0.6 | |
| Initial divergence | a' | 0..1 | 0.2 | |

Fig.3

WARNING! Window 3 displays input data for test example contained in *-IN file of the floppy disk delivered. While entering new input data in window 3 You overwrite old ones. Column "New Data" must be typed down all. By choosing ESC You get run test version with updated input data which do not correspond to information of column "Test" in the table of window 3. Therefore You may save time if You edit *-IN file before getting DYNAMIC.EXE run. In this case while being in window 3 You merely press ESC to perform test version with already updated input data.

WARNING! If current directory does not contain *-IN file, press ENTER and write input data from the screen.

2.4. The result of Program DYNAMIC run appears in window 4. It looks like Fig.4 for unit JET and like Fig.5 for unit PLASMOID. For more information about representation of the Program run results, see descriptions of Program units.

2.5. As the Program run is over, press ENTER to return to MENU in window 2. Here You may choose the new calculation version or escape Program DYNAMIC by pressing ESC.

# 3. Unit JET

## 3.1. Physical base

JET unit calculates characteristics of plasma jet free expansion in vacuum for plasma sources of steady state mode operation.

The general assumption is that two components plasma is fully ionized and its flow is adiabatic one.

Self-consistent plasma flow in a steady state axial symmetric jet is described with the set of equations using cylindrical coordinates x and r:

$$\frac{\partial nu}{\partial x} + \frac{\partial rnu}{r \partial r} = 0;$$

$$mn \left( u\frac{\partial u}{\partial x} + \nu\frac{\partial u}{\partial r} \right) = - \frac{\partial nT}{\partial x} ;$$

$$mn \left( u\frac{\partial \nu}{\partial x} + \nu\frac{\partial \nu}{\partial r} \right) = - \frac{\partial nT}{\partial r} ;$$

$$\frac{n}{\gamma-1} \left( u\frac{\partial T}{\partial x} + \nu\frac{\partial T}{\partial r} \right) + nT\left( \frac{\partial u}{\partial x} + \frac{\partial r\nu}{\partial r} \right) = \nabla q ,$$

The self-similar form of solution for the system (4) is written as:

$$u = u_c(x) \cdot y(\eta); \quad \nu = u \cdot da/dx \cdot \eta; \quad T = T_c(x) \cdot \tau(\eta); \quad nu = N\nu /\pi a^2 \cdot f(\eta),$$

$r = a(x)$ is a certain flow current line (see Fig. 4).

For three functions $u_c(x)$, $T_c(x)$ and $a(x)$ there are four equations:

$$\frac{mu_c^2}{2} + \frac{\gamma}{\gamma-1} T_c = const; \qquad \frac{mu_c a}{T_c} (u_c a')' = C_1;$$

$$T_c^{1/(\gamma-1)} \cdot u_c a^2 = const; \qquad \frac{T_c}{u_c} a^{(C_2-1)} = const;$$

where $C_1$ and $C_2$ are separation constants for variables x and $\eta$ correspondingly.

The latter is identical to the adiabatic equation when $u_c \rightarrow const$ and $C_2 = 2\gamma$. For adiabatic expansion the flow velocity always reaches its maximal value and remains practically constant, i.e.

$$u^2 \rightarrow u_m^2 = u_0^2 \, [1 + 2 \cdot M_0^{-2} \cdot (\gamma - 1)^{\gamma - 1}].$$

With $C_1 = C_2$, we obtain the following relationships for jet expansion along the axis:

$$u_c = u_m \; ; \quad T_c a^{2(\gamma - 1)} = T_0 a_0^{2(\gamma - 1)} \; ; \quad m u_m a a'' = 2 T_0 (a_0/a)^{2(\gamma - 1)} \quad (1)$$

For rarefied plasma flows with uniform temperature in the flow cross sectional plane in vicinity of the flow pole due to high thermal conductivity of the plasma $\partial T/\partial r = 0$, $T_c = T_c(x)$, the problem solution is written as:

$$n = \frac{N \cdot (\gamma - 1/2)}{\pi a^2 u_m} \frac{1}{(1 + r^2/a^2)} \; ; \quad u = \frac{u_m}{(1 + r^2/a^2)^{1/2}} \; ;$$

$$T = T_{co} \cdot (a_0/a)^{2(\gamma - 1)}; \quad a = a_0 + a_m (x - x_0) \; ; \quad (2)$$

$$a_m^2 = a_0^2 + 2/((\gamma - 1) \cdot M_0^2) \; ;$$

These formulas suggest that the distributions of plasma flow parameters in the far region of the jet where $a \gg a_0$ are defined by the particles flow rate, $N$, the ultimate plasma velocity, $u_m$, and the factor of flow divergency, $k = 1/(a'_m)^2$.

## 3.2 General Algorithm

The first step is calculation of profile of plasma jet characteristic transverse size ,a(x), along the jet axis, x, in the way of Kutta-Merson integration of the ordinary nonlinear differential equation (1). The input data are given at x=0: $a_0$ =1, $T_0$=1. Values of $\gamma$, $a_0$' и $M^2$ are specified by a user. A user also chooses mutually correlated integration step h and area s taking into account available PC capacity and display resolution. For instance if You specify s=10, the proper choice for h is 0.01 and 0.1 for s=100 to obtain curves capital enough on a screen and to save time run. The resultant values of a(x) at every integration step are collected in file A.OUT and corresponding values of x coordinate are stored in file S.OUT. These data are reserved for further use after Program run is over.

Integration run is stopped as condition x>s is satisfied and files A.OUT and S.OUT. become open for readout and use in calculation of spatial distributions of plasma concentration n(x) and temperature T(x) using expressions (2).

The expression for n(x) of set (2) is also used to calculate configuration of equal plasma concentration lines via variation of transverse coordinate r.

## 3.3 Input data

The calculations are run in the dimensionless form. The scale of linear dimensions is initial transverse size of the jet, $a_0$, and the temperature and plasma concentration scales are initial values $T_0$ and $n_0$.

Input parameters for JET unit are the following:

g = specific heat ratio $\gamma$;

M = Mach number;

h = integration step;

s = integration area along the jet axis;

$n/n_0$ = equal plasma concentration line parameter;

a' = flow divergence.


## 3.4 Input data ranges

| Identifier | Range | Note |
|:---:|:---:|:---|
| g | 1...5/3 | = 5/3 for test example |
| M | 2...15 | = 2.5 for test example |
| h | 0.001...1 | choice of correlation |
| s | 1...100 | between h and s   see 3.2 |
| n | 0.999...0.001 | = 0.8 and 0.6 for test example |
| a' | 0...1 | = 0.2 for test example |


## 3.5 Results description

Results of JET unit run are profile of plasma jet  characteristic transverse size ,a ,  along the jet axis,  x, spatial distributions of plasma concentration n(x) and temperature T(x) and equal  plasma concentration lines for two levels (0.8 and 0.6 for test example). Screen view is shown in Fig.  4.  The additional output information are  data saved in files A.OUT and S.OUT.
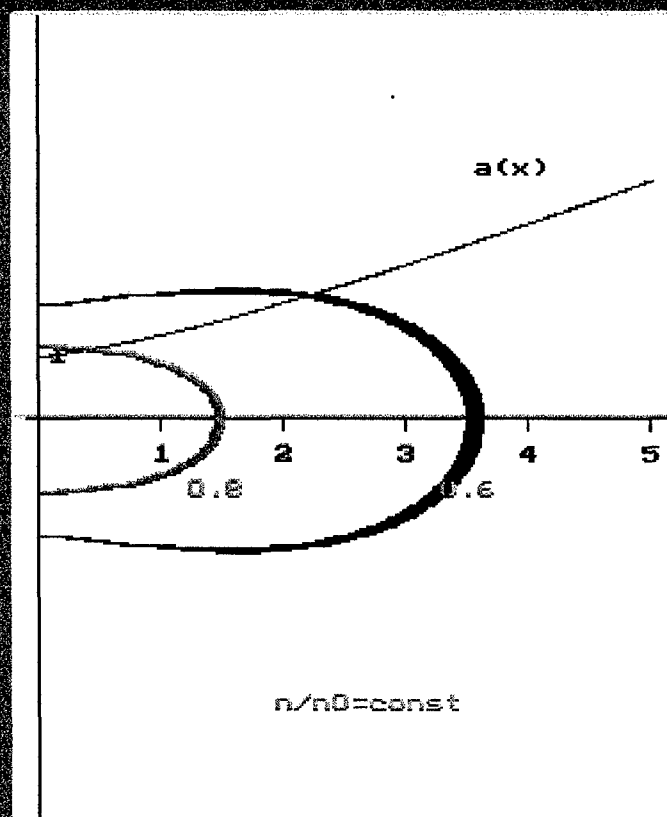
# CALCULATION OF JET CHARACTERISTICS



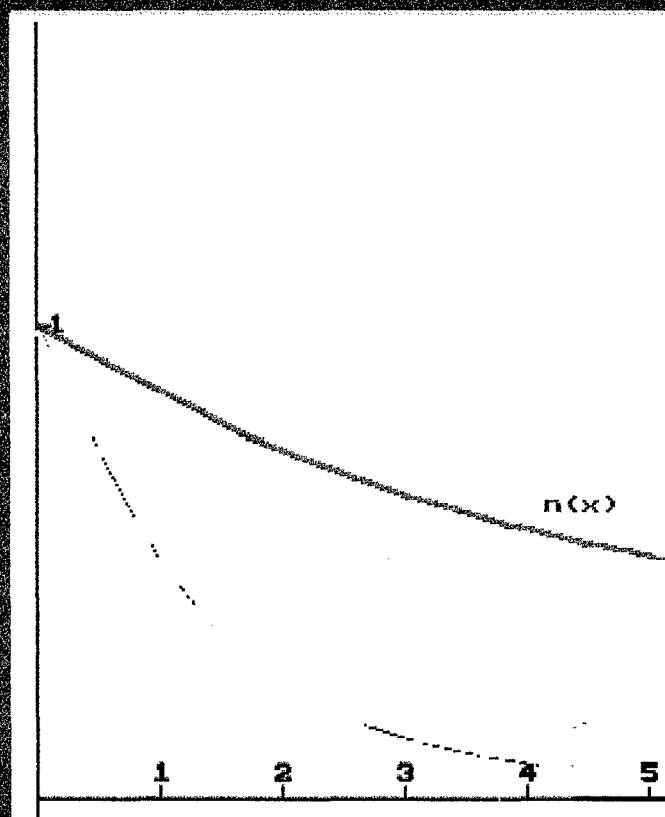Fig.1 Transverse size of Jet and equal concentration lines

Fig.2 Change of electron temperature and density along Jet axis

Fig.4

# 4. Unit PLASMOID.

## 4.1. Physical base

Unit PLASMOID calculates characteristics of plasmoid free expansion in vacuum for plasma sources of pulse mode operation.

For three-dimensional non-steady-state plasmoid the system of dynamic equations in Cartesian coordinates is written as:

$$\frac{\partial n}{\partial t} + \frac{\partial nu}{\partial x} + \frac{\partial n\nu}{\partial y} + \frac{\partial nw}{\partial z} = 0$$

$$mn \left( \frac{\partial u}{\partial t} + u \frac{\partial u}{\partial x} + \nu \frac{\partial u}{\partial y} + w \frac{\partial u}{\partial z} \right) + \frac{\partial nT}{\partial x} = 0$$

$$mn \left( \frac{\partial \nu}{\partial t} + u \frac{\partial \nu}{\partial x} + \nu \frac{\partial \nu}{\partial y} + w \frac{\partial \nu}{\partial z} \right) + \frac{\partial nT}{\partial y} = 0$$

$$mn \left( \frac{\partial w}{\partial t} + u \frac{\partial w}{\partial x} + \nu \frac{\partial w}{\partial y} + w \frac{\partial w}{\partial z} \right) + \frac{\partial nT}{\partial z} = 0$$

$$\frac{1}{\gamma - 1} n \left( \frac{\partial T}{\partial t} + u \frac{\partial T}{\partial x} + \nu \frac{\partial T}{\partial y} + w \frac{\partial T}{\partial z} \right) + nT \cdot \vec{\nabla} V = \vec{\nabla} q$$

Here $T = T_e + T_i$ is the sum of ion and electron temperatures. Assumed dependencies of velocities on coordinates are linear:

$$u = \overset{\bullet}{a} \frac{x}{a} \ ; \quad \nu = \overset{\bullet}{b} \frac{y}{b} \ ; \quad w = \overset{\bullet}{c} \frac{z}{c}$$

where $a = a(t)$, $b = b(t)$ $c = c(t)$ are characteristic sizes of the plasmoid along axes $x, y, z$ respectively. Spatial distribution of plasma concentration and temperature within a plasmoid is written as:

$$n = \frac{N \nu}{8abc} \cdot f_1(\eta) f_2(\xi) f_3(\zeta) \ ; \tag{3}$$

$$T = T_c(x) \ \tau \ ( \ \eta, \ \xi, \ \zeta \ )$$

where $\nu$ is a normalization factor defined from the integral

$$\int\int\int_{\infty}^{\infty} n \ dxdydz = N,$$

where $N$ is the total amount of particles in the plasmoid, and $f_1$, $f_2$ and $f_3$ are functions of self-similar variables $\eta = \dfrac{x}{a} \ ; \xi = \dfrac{y}{b} \ ; \zeta = \dfrac{z}{c}$

such that $f_1(0) = f_2(0) = f_3(0) = 1$.

The representative solution corresponds to the case of uniform temperature throughout the plasmoid e.i. $\tau = 1$ and $\nabla q = 0$. This case is realized for "hot" plasmoid when the role of heat conductivity in plasma is sufficient, especially under condition of no energy exchange between the plasmoid and the environment. In this case:

$$f_1 = \exp\left(-\frac{x^2}{2a^2}\cdot C_1\right); \quad f_2 = \exp\left(-\frac{y^2}{2b^2}\cdot C_2\right); \quad f_3 = \exp\left(-\frac{z^2}{2c^2}\cdot C_3\right); \quad (4)$$

Characteristic sizes of a, b, c are specified as those ones corresponding to "knee" in dependence of n on coordinates and to the condition:

$$f_1{}''(1) = f_2{}''(1) = f_3{}''(1) = 0$$

The separation constants can be also determined from these condition:

$$C_1 = C_2 = C_3 = 1$$

For a "heat insulated" plasmoid with uniform temperature the energy equation (3) is reduced to the adiabatic relationship:

$$T_c = T_0 \left(\frac{n}{n_0}\right)^{\gamma-1} = T_0 \left(\frac{a_0\, b_0\, c_0}{a\, b\, c}\right)^{\gamma-1} \quad (5)$$

For definition of time dependent sizes of the plasmoid there is a set of non-linear differential equations :

$$ma\ddot{a} = mb\ddot{b} = mc\ddot{c} = T_0 \left(\frac{a_0\ b_0\ c_0}{a\ b\ c}\right)^{\gamma-1} \quad (6)$$

Here dots denote derivatives with respect to time, t. The characteristic property of this three-dimensional expansion is non-uniform increase of plasmoid sizes. If initial velocities are low compared to the mean random velocity, $v_T \sim \sqrt{T_0/m}$, the resulting velocity is maximal along the coordinate where the initial size of a plasmoid is minimal. Consequently resulting size of a plasmoid along this coordinate finally occurs to be maximal. So inversion of sizes takes place.

For example, a plasmoid initially generated as a "knitting need-

le" stretched along axis x, later transforms in a disk with minimal x dimension. In contrary a dense disk may transform in a long "knitting needle". The reason of this inversion is clear enough: the thermal energy initially accumulated by a plasmoid, gradually transforms in kinetic energy of expansion predominantly in the direction of maximal gradient of electric potential or in other words along the maximal gradient of total inner pressure $\nabla(nT_i + nT_e) \approx \nabla nT_i + en\nabla\Phi$ .

## 4.2 General Algorithm

The first step is calculation of temporal dependencies of plasmoid linear dimensions $a(t)$, $b(t)$ and $c(t)$ in the way of Kutta-Merson integration of combined ordinary nonlinear differential equations (6). The input data are given at $t=0$: $T_0=1$, $m_0=1$, $a_0'=b_0'=c_0'=0$. Values of $\gamma$, M, $a_0$, $b_0$, $c_0$ are specified by a user. A user also chooses mutually correlated integration step h and temporal area t taking into account available PC capacity and display resolution. For instance if You specify $t=10$, the proper choice for h is 0.01 and 0.1 for $t=100$ to obtain curves capital enough on a screen and to save time run. The resultant values of $a(t)$, $b(t)$ and $c(t)$ as well as derivatives $a'(t)$, $b'(t)$ and $c'(t)$ at every integration step are collected in files A.OUT B.OUT and C.OUT, A1.OUT B1.OUT and C1.OUT correspondingly whereas values of "t coordinate" are stored in file T.OUT. These data are reserved for further use after Program run is over.

Integration run is stopped as condition $t>\tau$ is satisfied and files A.OUT B.OUT and C.OUT, A1.OUT B1.OUT and C1.OUT become open for readout and use in calculation of temporal distributions of plasma temperature $T(t)$ and concentration $n(t)$ at the plasmoid center using expressions (5) and (3) combined with (4) correspondingly .

The expression (3) combined with (4) is also used to calculate configuration of equal plasma concentration lines of $n/n_0 = 0.5$ level for two fixed moments $t_1=50\cdot h$ and $t_2=500\cdot h$.


## 4.3 Input data

The calculations are run in the dimensionless form. The scale of linear dimensions is initial maximal size of the plasmoid, $a_0$. Generally the plasmoid is characterized with three initial sizes - maximal, mean and minimal. In the test example the plasmoid is initially

an elliptic cylinder with the maximal size being tenwise greater than the minimal one. The temperature and plasma concentration scales are initial values, $T_0$ and $n_0$. Values of $t_0 = \sqrt{m a_0^2 / T_0}$ is the temporal scale.

Input parameters for PLASMOID unit are the following:

a0 = maximal initial size;

b0 = mean initial size;

c0 = minimal initial size;

g = specific heat ratio $\gamma$;

h = integration step;

t = duration of free expansion.

## 4.4 Input data ranges

| Identifier | Range | Note |
|---|---|---|
| a0 | 0...1 | = 1.0 for test example |
| b0 | 0...1 | = 0.2 for test example |
| c0 | 0...1 | = 0.02 for test example |
| h | 0.001...1 | choice of correlation |
| t | 1...100 | between h and t see 4.2 |
| g | 1...5/3 | = 5/3 for test example |

## 4.5 Results description

Results of PLASMOID unit run are the following (screen view is shown in Fig.5) :

- time profiles of three characteristic sizes and three velocity components of the plasmoid; ('Fig.1')

- time profile of plasma concentration and temperature in the center of the plasmoid; ('Fig.2')

- coordinate profiles of plasma concentration for moment $t_2$:

- line of equal concentration in coordinate planes for moments $t_1$ and $t_2$ - $n/n_c$ =0.5. ('Fig.4,5')

The additional output information are data saved in files *.OUT.
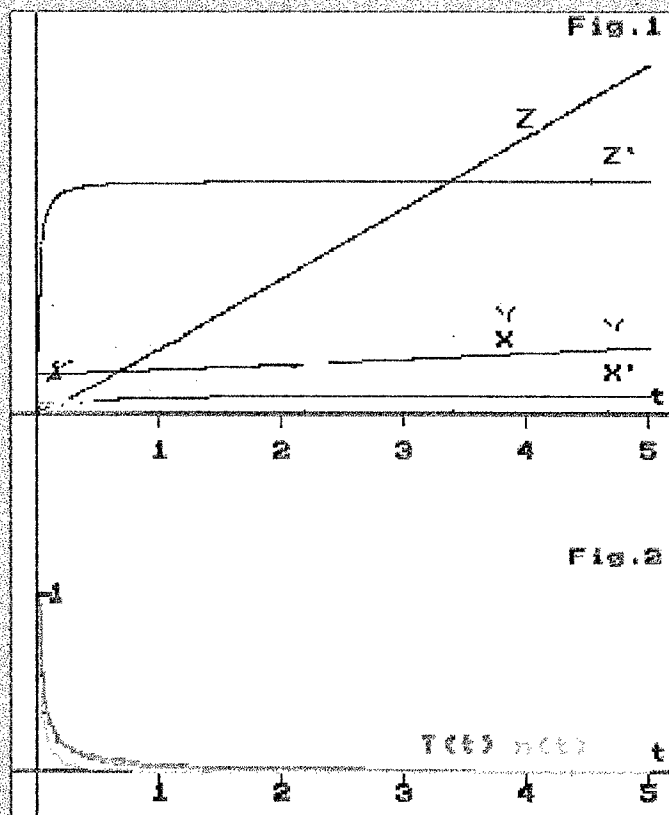


Fig.1 Linear sizes and velocity components

Fig.2 Change of electron temperature and density in centre
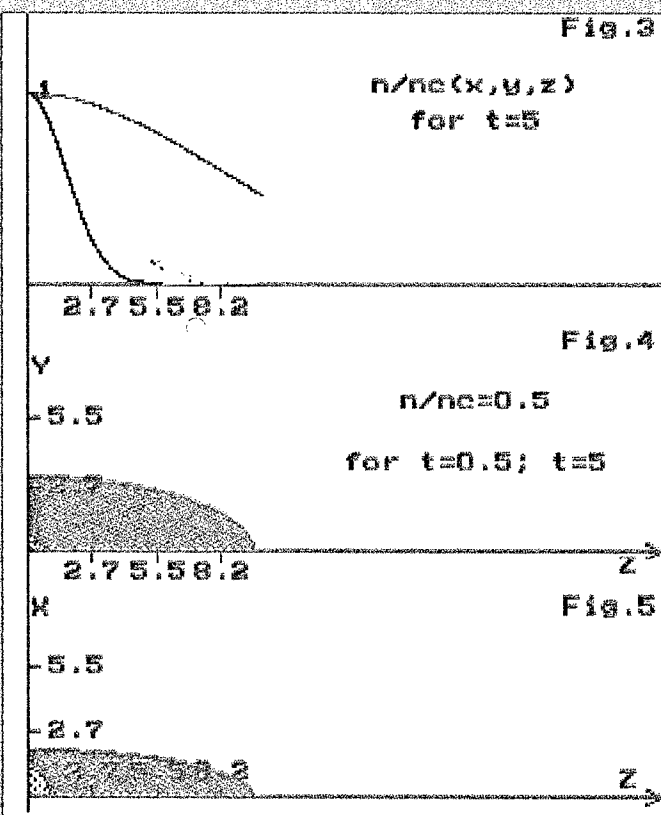
Fig.3 Distribution of electron density along axises X,Y,Z

Fig.4,5 Plasmoid cross-sections

Fig.5

## Proposals

## on further stages

## of Development of dynamical and mathematical models

## of plasma flows in space

## with due regard for action the Earth magnetic field.

This Appendix submits a set of new proposals for EOARD that could be a perspective of future cooperation. This set encloses a part of our professional interests where we have a sufficient theoretical and experimental background.

The proposals submitted are based on the main principle that every given proposal covers one or a number solved problem as a final result available for a user. As a rule validity of this result is evaluated by the way of comparison with in-house experimental and/or published data.

The set of given new proposals concerns three types of artificial plasma formations (APFs) which can arise in space particularly in vicinity of a spacecraft as a typical result of normal operation of certain onboard systems or may be intently created for scientific or applied goals: stationary plasma plumes, plasmoids or ionized clouds and gas-plasma formations as a result of natural ionization of neutral gas releases. Adequate description and parameters calculation of every APF type presents an independent chain of dynamical problems, methods and codes. Every chain is multi-link since for every APF type one may define a few (2 – 4) stages of expansion in dependence on predominant mechanisms and degree of interaction of injected substance with main dynamical factors of space flight, namely the Earth magnetic field and environment.

The first stage corresponds to non-perturbed expansion of dense plasma flow core where the plasma density and pressure are much greater than the density of environmental media and magnetic pressure. This stage is characterized by inertial axissymmetric expansion of a plasma plume and almost spherical expansion of a plasmoid moving with any drift velocity. In other words the artificial plasma at this stage does not "feel" neither magnetic field nor environment so that only inner electric fields control the plasma flow.

In gas releases non-elastic collisional processes including ionization and excitation are sufficient at the first stage of expansion.

The second stage of flow expansion corresponds to the condition when magnetic pressure already exceeds that one of plasma whereas the density of the latter is still sufficiently greater than environmental density so that the movement of particles conserves collective character and plasma expansion across the magnetic field is inhibited. As a result the plasma plume obtains a form of three dimensional "petal" and the plasmoid becomes "a knitting needle" stretched along the magnetic field.

At the third stage the movement of plasma particles becomes non-collective and is completely controlled by external natural fields and interaction with environmental particles. This region may be treated as a "trace" of the injection which used "to live" for a relatively long time. This is a weak but large inhomogenity usually interesting for geophysists which love active experiments in space. One may expect that this region is also responsible for return fluxes of injected particles to the spacecraft. We have made a brief analyses on dynamics of the third stage of plasma expansion in connection with interpretation of certain our previous space experiments. This approach if being interesting could be also a base of future cooperation.

For typical injections of modest intensity (flow rates of $10^{19}$ – $10^{21}$ particles per second and $10^{20}$ – $10^{22}$ per pulse) the characteristic dimensions of the first stage of flow ranges up to ten meters, of the second stage – from a few tens to a few hundreds meters and of the third stage – from a few hundreds to a few thousand meters.

Our experience (and not only ours) suggests that attempt to formulate unitary dynamic problem for all stages of APF expansion results in large non-visual and inconvenient algorithms of enormous run times. Much more effective way is formulation and solution of separate dynamical problems for every stage of expansion of every APF type.

Such an approach results in relatively compact visual solutions suitable either for "intuitive" analyses or numerical calculation.

While speaking about dynamical and mathematical models of APF we actually separates two distinct phases in the procedure of dynamic problem formulation and solution.

The first phase encloses evaluation of acting forces and "dynamical range" of the problem, consequent reduction of the initial set of equations to a final dimensionless form convenient for solution .

The second phase results in an analytical solution of the problem and/or in a code for numerical calculation. Surely it is the general routine of dynamical problem solution. With this separation of the routine in two phases we'd like to underline that principally there is or may be a few ways to obtain the mathematical result basing on the same or similar dynamical model.

In the ranges of our interests the APF mathematical models are

mainly used for description and study of radio frequency (RF) refraction/scattering effects. The base of scattering calculations is the ordinary method of the eikonal equation numerical solution with dielectric permeability being expressed via electron density distribution. Method of linearization for the eikonal initial set of characteristic equations now under development allows for sufficient reduction of run time.

For every APF type and for every stage of expansion we'd like to present the following PC codes:

      *spatial intensity distribution of scattered spherical wave

          (usable example gratias for evaluation of communication

          conditions along the line "board - the Earth");

     **spatial intensity distribution of scattered plane wave

          (the same for the line "the Earth - board");

    ***cross section of backward scattering

          (usable for evaluation of observation conditions).

Although the similar approaches are used in development of all these codes, every one is the separate independent program product since it includes its own APF model and utilizes its own way of optimization.

Further symbols *, **, *** are used to denote the code type.

The works mentioned above may be displayed with the scheme:

```
                    ┌──────────────────────────┐
                    │        Artificial        │
                    │     Plasma  Formations    │
                    └──────────────────────────┘
        ┌──────────────────────┼──────────────────────┐
┌──────────────────┐  ┌──────────────────┐  ┌──────────────────┐
│ stationary plasma│  │  plasmoids or    │  │   gas-plasma     │
│     plumes       │  │ ionized clouds   │  │   formations     │
└──────────────────┘  └──────────────────┘  └──────────────────┘
```

D          Y          N          A          M          I          C          S

(   dynamical   and   mathematical   models   of   APFs   )

```
┌────────────┐  ┌────────────┐  ┌────────────┐  ┌────────────┐  ┌────────────┐
│  work1-94  │  │  work3-95  │  │  work1-94  │  │  work7-97  │  │  work2-94  │
│   dense    │  │3-dimensi-  │  │   dense    │  │  knitting  │  │  ionized   │
│   core     │  │onal petal  │  │   core     │  │  needle    │  │   jet      │
│SPC-94-4081 │  │            │  │SPC-94-4081 │  │            │  │SPC-94-4080 │
└────────────┘  └────────────┘  └────────────┘  └────────────┘  └────────────┘
```

RADIO    FREQUENCY    SCATTERING / REFRACTION    CHARACTERISTICS

(algorithms and PC codes)

```
┌──────────────────────────────────────┐
│              work4-95                 │
│  linearization of eikonal equation    │
└──────────────────────────────────────┘
┌────────────┐  ┌────────────┐     ┌────────────┐   ┌────────────┐
│  work4-95  │  │  work6-96  │     │  work8-97  │   │  work9-97  │
│   code:    │  │   codes:   │     │   codes:   │   │   codes:   │
│    *       │  │    *       │     │    *       │   │    *       │
│            │  │     **     │     │     **     │   │     **     │
│            │  │      ***   │     │      ***   │   │            │
└────────────┘  └────────────┘     └────────────┘   └────────────┘
┌────────────┐
│  work5-96  │
│   codes:   │
│    **      │
│      ***   │
└────────────┘
```

This scheme also shows our proposal on annual distribution of the works mentioned above with account for the contracts in force and actual volume of work.

Finally we propose the following annual distribution of the works.

## Contracts of 1994 in force

~25000$    work1-94    Dynamical and mathematical models of

          SPC-94-4081    plume and plasmoid dense core ;

20000$    work2-94    Dynamical and mathematical model of

          SPC-94-4080    ionized jet.

- o -

## Proposed contracts of 1995

~23000$    work3-95    Dynamical and mathematical model of

                          3-dimensional plasma petal;

~23000$    work4-95    Linearization of eikonal equation

                          and code * for plume dense core;

## Proposed contracts of 1996

work5-96    Codes * and ** for plume dense core;

work6-96    Codes *, ** and ***

                      for 3-dimensional plasma petal;

(This contracts being fulfilled close the vertical chains on plume dense core and 3-dimensional plasma petal the scheme presented above).

## Proposed contracts of 1997

|         |                                                          |
|---------|----------------------------------------------------------|
| work7-97 | Dynamical and mathematical model of 3-dimensional knitting needle; |
| work8-97 | Codes *, ** and *** for 3-dimensional knitting needle; |
| work9-97 | Codes *, ** and ** for ionized jet; |

(This contracts being fulfilled close the vertical chains on plasmoids and ionized jets).

At the bottom line we propose two works for 1995 – one on dynamics and one on scattering , also two works for 1996 – both on scattering and three works for 1997 – one on dynamics and two on scattering.